AD-782 036

CHALCOGENIDE GLASSES FOR HIGH ENERGY LASER APPLICATION

A. R. Hilton, et al

Texas Instruments, Incorporated

Prepared for:

Office of Naval Research
Advanced Research Projects Agency

June 1974

DISTRIBUTED BY:

NTIS

National Technical Information Service
U. S. DEPARTMENT OF COMMERCE
5285 Port Royal Road, Springfield Va. 22151

UNCLASSIFIED

Security Classification

AD-782 036

DOCUMENT CONTROL DATA - R & D

(Security classification of title, body of abstract and indexing annotation must be entered when the overall report is classified)

1. ORIGINATING ACTIVITY (Corporate author) Texas Instruments Incorporated Central Research Laboratories 13500 North Central Expressway Dallas, Texas 75222	2a. REPORT SECURITY CLASSIFICATION UNCLASSIFIED 2b. GROUP --

3. REPORT TITLE

Chalcogenide Glasses for High Energy Laser Applications

4. DESCRIPTIVE NOTES (Type of report and inclusive dates)

Final Technical Report, 1 May 1973 through 30 April 1974

5. AUTHOR(S) (First name, middle initial, last name)

A. R. Hilton
D. J. Hayes
M. D. Rechtin

6. REPORT DATE	7a. TOTAL NO. OF PAGES	7b. NO. OF REFS
June 1974	76	34

8a. CONTRACT OR GRANT NO N00014-73-C-0367 b. PROJECT NO c. ARPA Order No. 2443 d. Program Code No. 3D10	9a. ORIGINATOR'S REPORT NUMBER(S) 08-74-44 9b. OTHER REPORT NO(S) (Any other numbers that may be assigned this report)

10. DISTRIBUTION STATEMENT

11. SUPPLEMENTARY NOTES	12. SPONSORING MILITARY ACTIVITY
	Advanced Research Projects Agency Washington, D. C.

13. ABSTRACT

New compounding techniques were devised to prep[are] high purity TI #1173 ($Ge_{28}Sb_{12}Se_{60}$) and TI #20 ($Ge_{33}As_{12}Se_{55}$). The methods were based on the combination of the reactant purification and compounding steps. The goal of the program was to establish the absorption limit for the glasses and to lower the absorption at 10.6 μm. At the present purity level, the Ge-Sb-Se glass is found to have an absorption level of about 0.01 cm^{-1} at 10.6 μm, while the absorption level for the Ge-As-Se glass is 0.05 cm^{-1}. Underlying causes for the limits are discussed, along with the possibilities for improvement.

Glasses based on sulfur and selenium were carefully characterized to establish the interdependence between chemical composition and the magnitudes of physical parameters related to their use as infrared optical materials. Parameters considered in this program were density, volume expansion coefficient, glass transition temperature, thermal conductivity, hardness, elastic moduli, and Poisson's ratio. The interdependence information will serve as a guide in selecting new sulfur-based glass compositions for development.

The sulfur glasses selected for evaluation were from the Ge-Sb-S system. A rather large glass-forming composition region was determined through the preparation of small laboratory samples. The physical properties of sulfur glasses were substantially better than those of the selenium glasses. Visible transmission was found for glasses containing 60 or more atomic percent sulfur. However, at their present state of purity, the Ge-Sb-S glasses are found to have an absorption at 10.6 μm of about 0.5 cm^{-1}, with the intrinsic limit estimated to be of the order of 0.1 to 0.05 cm^{-1}. Chalcogenide glasses do not appear promising as high energy CO_2 laser window materials.

DD FORM 1 NOV 65 1473

UNCLASSIFIED

Security Classification

UNCLASSIFIED
Security Classification

14. KEY WORDS	LINK A		LINK B		LINK C	
	ROLE	WT	ROLE	WT	ROLE	WT
Infrared transmitting glasses						
Absorption in chalcogenide glasses						
Interdependence of physical parameters for infrared transmitting glasses						
High-purity selenium-based glasses						
Low-loss acoustic materials						

ia

UNCLASSIFIED
Security Classification

TI Report No.
08-74-44

CHALCOGENIDE GLASSES FOR HIGH ENERGY LASER APPLICATIONS

Contract No. N00014-73-C-0367

A. R. Hilton

D. J. Hayes

M. D. Rechtin

Texas Instruments Incorporated

Final Technical Report

June 1974

Sponsored by
Advanced Research Projects Agency
ARPA Order No. 2443

ARPA Order Number:	2443
Program Code Number:	3D10
Name of Contractor:	Texas Instruments Incorporated Central Research Laboratories P. O. Box 5936 Dallas, Texas 75222
Effective Date of Contract:	1 May 1973
Contract Expiration Date:	30 April 1974
Amount of Contract:	$72,260
Contract Number:	N00014-73-C-0367
Principal Investigator and Phone No.:	A. Ray Hilton (214) 238-2596
Scientific Officer:	Director, Metallurgy Programs Material Sciences Division Office of Naval Research Department of the Navy 800 North Quincy Street Arlington, Virginia 22217
Short Title of Work:	Glass IR Window

PROGRAM SUMMARY

New compounding techniques were devised to prepare high purity TI #1173 ($Ge_{28}Sb_{12}Se_{60}$) and TI #20 ($Ge_{33}As_{12}Se_{55}$). The methods were based on the combination of the reactant purification and compounding steps. The goal of the program was to establish the absorption limit for the glasses and to lower the absorption at 10.6 μm. At the present purity level, the Ge-Sb-Se glass is found to have an absorption level of about 0.01 cm^{-1} at 10.6 μm, while the absorption level for the Ge-As-Se glass is 0.05 cm^{-1}. Underlying causes for the limits are discussed, along with the possibilities for improvement.

Glasses based on sulfur and selenium were carefully characterized to establish the interdependence between chemical composition and the magnitudes of physical parameters related to their use as infrared optical materials. Parameters considered in this program were density, volume expansion coefficient, glass transition temperature, thermal conductivity, hardness, elastic moduli, and Poisson's ratio. The interdependence information will serve as a guide in selecting new sulfur-based glass compositions for development.

The sulfur glasses selected for evaluation were from the Ge-Sb-S system. A rather large glass-forming composition region was determined through the preparation of small laboratory samples. The physical properties of sulfur glasses were substantially better than those of the selenium glasses. Visible transmission was found for glasses containing 60 or more atomic percent sulfur. However, at their present state of purity, the Ge-Sb-S glasses are found to have an absorption at 10.6 μm of about 0.5 cm^{-1}, with the intrinsic limit estimated to be of the order of 0.1 to 0.05 cm^{-1}. Chalcogenide glasses do not appear promising as high energy CO_2 laser window materials.

TABLE OF CONTENTS

Preceding page blank

TABLE OF CONTENTS

(continued)

LIST OF TABLES

LIST OF ILLUSTRATIONS

LIST OF ILLUSTRATIONS

(continued)

SECTION I

INTRODUCTION

Infrared transmitting glasses based on the chalcogen elements sulfur, selenium and tellurium have been under investigation at Texas Instruments since 1961.[1] Two glass compositions, TI #1173 ($Ge_{28}Sb_{12}Se_{60}$) and TI #20 ($Ge_{33}As_{12}Se_{55}$) have emerged from this investigation. These glasses have been produced in commercial quantities and used to fabricate optical elements for use in infrared optical systems. Recently,[2,3] considerable attention has been given to the problem of finding infrared optical materials with properties suitable for use with high energy CO_2 lasers emitting at 10.6 μm. Each material considered is found to have its own set of advantages and disadvantages.[4,5] For existing chalcogenide glasses, the thermal conductivity is found to be an order of magnitude too low, while the absorption at 10.6 μm is two orders of magnitude too high. The purpose of this program was to investigate the possibilities of preparing chalcogenide glasses better suited for use with high energy CO_2 lasers.

The low values for thermal conductivity in TI #1173 and TI #20 reflect the disordered nature of the glasses and therefore cannot be improved. However, if the absorption at 10.6 μm reflects a quality state of the glass (extrinsic limitation) rather than an intrinsic limit, considerable improvement may be realized through increasing the purity of the glasses. Section II of this report describes attempts in this laboratory to establish the intrinsic limit for TI #1173 and TI #20.

Several years ago when numerous chalcogenide glass-forming systems were evaluated, selection of the glass composition for development was based on evaluation with regard to only a few parameters. Within a glass-forming system, the ratios between the constituent elements may vary greatly and the associated physical properties of the resultant glasses may be expected to vary as well.

It is reasonable to assume that if all the pertinent physical parameters are considered, glass-forming systems can be reevaluated and a new glass composition selected with properties better suited for application with CO_2 lasers. The interdependence of the pertinent physical parameters and how they change with composition must serve as a guide in the selection of a new composition. Data for the physical properties of various selenium-based and sulfur-based glasses are presented in Section III of this report.

The final goal of this program was to select for evaluation one or two glass compositions based on the element sulfur in place of selenium. Physical properties related to use with CO_2 lasers (thermal conductivity, thermal volume expansion coefficient, thermal change in refractive index, etc.) could be expected to improve. The results obtained in the complete evaluation of the Ge-Sb-S system are presented in Section IV.

SECTION II

INFRARED ABSORPTION OF HIGH PURITY TI #1173 AND TI #20

A. Evaluation Methods

1. Trace Impurity Evaluation

a. Emission Spectrograph

Trace metallic impurities in solids are generally determined in this laboratory using a Baird Atomic GX-1 three-meter grating (30,000 grooves/inch) emission spectrograph. High purity Poco Graphite electrodes are used, leading to a detection limit of 0.1 to 10 ppm/weight for most common metallic elements. Trace anion impurities such as Cl^-, Br^-, or OH^-, along with negative elements such as S, Se, or Te, are not ordinarily detected (unless they are present as a major constituent).

b. Infrared Absorptions by Oxides

Semiconductor solids transparent in the infrared show absorption characteristic of oxide impurities present within the bulk. Classic examples are silicon (9.5 μm) and germanium (11.6 μm).[6] The magnitude of the absorption coefficient can be used to estimate the concentration of oxygen present[6] in the reactant germanium. Bands characteristic of oxides in selenium have also been reported in the literature.[7] However, neither antimony nor arsenic, the other reactants, transmit in the infrared. For the compounded glasses, TI #1173 and TI #20, infrared transmission is routinely used to estimate the bulk oxide concentration.[8] A nomograph relating the transmission at 13 μm for both glass compositions was prepared[8] from the measured transmission of glasses doped with various amounts of SeO_2.

c. Neutron Activation Analysis

Recently,[9] workers using activation analysis techniques have been able to go well beyond the sensitivity limit (2 ppm) of the infrared transmission method in silicon down to the low ppb range. The method used is general and can be applied to other solids, provided that suitable samples can be obtained and that an etch suitable for removal of surface oxides is employed. The methods, developed by the staff of the center for Material Trace Characterization, Department of Chemistry, Texas A&M University, were employed in this investigation to verify the accuracy of the infrared transmission method used for compounded glasses.

2. Optical Evaluation

a. Infrared Transmission

Two optical null double-beam infrared spectrophotometers were used to measure infrared transmission of polished glass samples: Perkin-Elmer Model 337 and a Perkin-Elmer Model 221 (with transmission scale expansion). According to the manufacturer, both instruments will yield better than 1% transmission accuracy. However, for low absorption - high refractive index materials, this accuracy cannot be maintained. To measure an appreciable change in transmission, the samples must be thick, which leads to an increase in the optical path on the sample side. Consequently, the optical image of the globar source on the active area of the detector is defocussed, resulting in an inaccurate comparison of I to I_0. The degree of the inaccuracy is a variable, depending on the instrument design and on the refractive index and the thickness of the sample.

The Perkin-Elmer 337 covers the range from 2.5 to 25 μm with transmission recorded on standard paper, which is stored in looseleaf notebooks

for reference. The Perkin-Elmer 221 has a relatively long focal length optical system (long relative to the Perkin-Elmer 337) and therefore yields more accurate transmission values for the thick glass samples. The expanded transmission scale feature (5X, 10X, and 20X) is an advantage in trying to estimate the absolute transmission for a sample when the absorption is a few percent or less. However, the scale factors quoted by the manufacturer must be checked by comparing transmission values for the same sample in low absorption regions recorded while using 1 x %T, 5 x %T, etc., so that the real values for 5, 10, or 20 can be calculated. The ability to calculate the absorption-free transmission values from the precise five-number refractive indexes for the TI #1173 and TI #20 glasses[10] has been very helpful in this program. In this way, the validity of the high transmission - very low absorption values can be judged.

The full transmission relationship for transparent materials is used:

$$T = \frac{(1-R)^2 e^{-\beta x}}{1-R^2 e^{-2\beta x}} ,$$

where T = transmission (I/I_o),

R = reflectivity,

β = bulk absorption coefficient, and

x = thickness of the sample.

A third source of transmission values was derived from the use of a Perkin-Elmer E-1 monochromator. A globar source is used with a thermocouple detector and a Perkin-Elmer lock-in amplifier. The usefulness of this system is its better spectral resolution, particularly at longer wavelengths,

and the ability to use dewars for transmission as a function of wavelength. The disadvantages are that the measurements must be made single-beam, point by point, and that there is an inherent accuracy limitation in using an electrical signal instrument as opposed to an optical null.

b. Laser Calorimetry

The most convenient method used for measuring low-level absorption by most investigators for 10.6 μm values is the laser calorimeter. The system used in this laboratory employs a single-mode, 50-watt Perkin-Elmer #6200 CO_2 laser. Incident powers from 7 to 15 watts have been used. The sample can be removed from the path for power settings. Measurements have been made both in air and under reduced pressure, with results in air giving slightly lower values. Both the adiabatic technique as described by Hass[11] and the steady state technique[12] have given comparable results; however, the steady state method is more convenient and is the one used. Samples are core-drilled about 1.1 inch in diameter and about 0.5 to 0.6 inch thick. They have a small 40-mil hole cavitroned in the side for a 5-mil diameter copper-constantan thermocouple. The hole is about 0.1 inch deep and is filled with a special thermal conducting grease to promote good heat transfer. The faces of each sample are polished plane and parallel using a Buhler Vibromet polisher and the usual alumina fine-grain polishing compounds.

c. Infrared Microscopy

A Research Devices Incorporated Model D infrared microscope has been invaluable in evaluating the quality of the infrared glass samples. The microscope is equipped with a Polaroid camera so that a permanent record can be made of infrared (~ 1.1 μm wavelength) images up to 430X taken in transmission or with reflected light. The instrument has been used to verify the removal of carbon particles from the glass or to investigate the possibility of crystallite formation.

B. Glass Preparation

1. Production Area Methods

a. Reactant Purification

The stated purity of reactants used in compounding glasses may be as high as six-nines. However, the purity figure does not include surface oxides. All reactants (except germanium, which is used in bar form) are treated in a similar manner to sublime the volatile surface oxides from the surfaces. Sublimation is carried out in cleaned glass or quartz tubes using flowing gas or reduced pressure to promote the separation. Temperatures are 300°C for selenium, 700°C for antimony, and 600°C for arsenic. Care is taken to minimize exposure of the purified reactants to moist air before use. The reactants are used almost immediately after purification.

Infrared transmission of polished samples of the germanium used for the glass preparation indicate the actual bulk oxygen concentration value is 0.2 to 0.3 ppm. Infrared transmission of a polished amorphous selenium sample showed no detectable selenium oxide absorption according to the absorptions reported by Vasko.[7]

b. Compounding

Quantities large enough for a 4 to 5 kgm batch of glass are weighed out; broken up using a large mechanical grinder; and placed in large, clean, high-purity quartz tubes. The entire amount is heated slightly (~ 200°C) and sealed off at reduced pressure. The tubes are placed in a rocking furnace, brought up to 800°C, and reacted for about 18 to 24 hours. Air-quenching from 575°C is used.

c. Casting

Bulk pieces of glass are placed in a large, resistive-heated, beaker-shaped furnace to provide glass for the plate to be cast. The furnace is in a large metal chamber that has been filled with forming gas (10% H_2, 90% N_2). The glass is melted and stirred from above at a temperature of about 600 to 650°C, cooled down to 575°C, and cast into a heated mold. The oxide impurity level for the cast glass is found to increase slightly from that of the compounded glass due to increased exposure. The production area oxide impurity level as estimated by the infrared transmission measurement[8] at 13 μm averages 3 to 5 ppm.

2. New Methods - Combination of Purification and Compounding Steps

Examination of the steps followed in the production process indicated that exposure to air after purification and during the casting operation led to an increase in the oxide concentration. A combination of the first two steps formed the basis for the methods used in this program. Casting was considered a problem separate from the purity problem, a problem that could be overcome whenever large plates were required. It was therefore decided to restrict attention to 1 kgm quantities and to cut and polish small samples from the 1 kgm boule for evaluation. The procedure is illustrated in the following figures.

Figure 1 diagrams the procedure followed in purifying the reactants. Three (or two) separate chambers are provided. The two outside chambers contain selenium and antimony (or arsenic). The center chamber contains the germanium and serves as the compounding chamber. Porous quartz frits are used to filter particulate matter when a reactant is distilled into the center chamber. This step is absolutely essential for the selenium, since (as reported previously[8]) the as-received material has been shown to contain amorphous carbon.

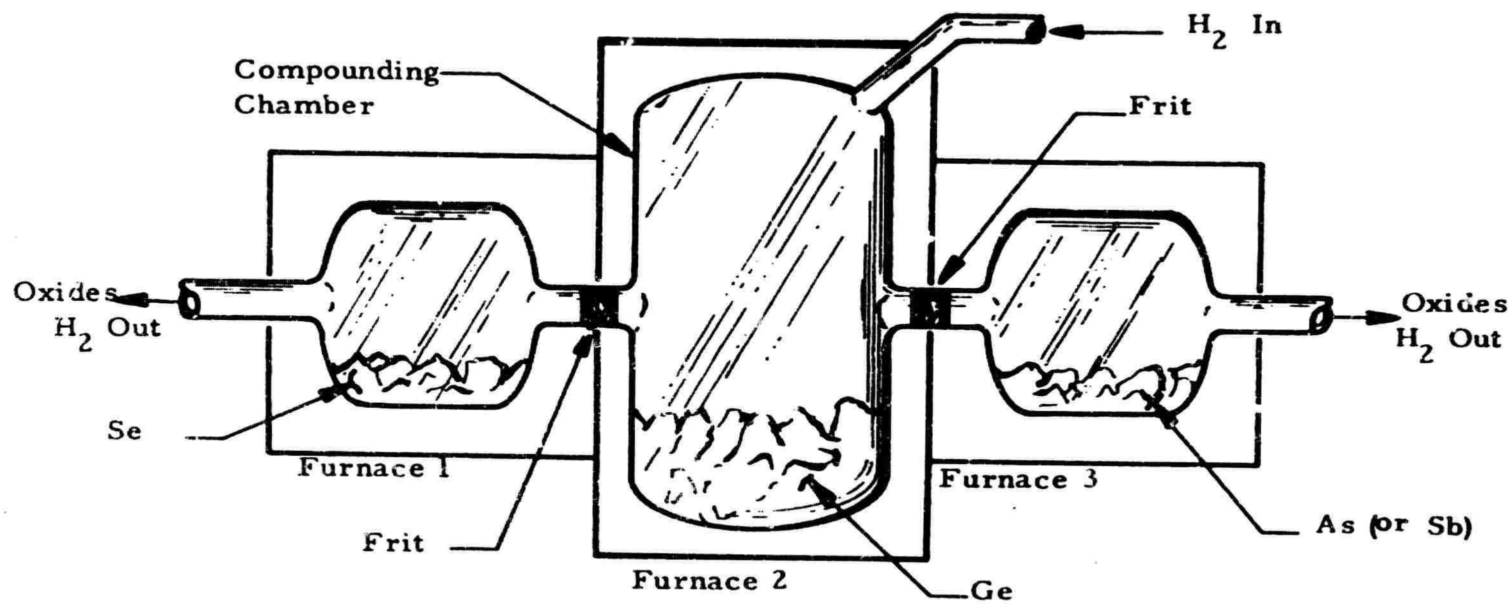

Figure 1 Diagram Depicting Process for Reactant Purification Step

Prior to placing the reactants in the chambers, the chambers were etched, dried, and placed in their respective furnaces. With a dry, oxygen-free gas (generally hydrogen) flowing through, all three chambers and the frits are heated to 800°C and flushed overnight to drive moisture from the quartz. The chamber is then cooled with an inert gas present (nitrogen or helium). The reactants are added, and the surface oxide treatment is begun. A temperature of 300°C is used for the selenium, 700°C for the antimony and germanium, and 350°C for the arsenic. The process is run overnight, covering a period of 16 to 18 hours.

The seal-off procedure and the distillation are depicted in Figure 2. The ends of the reactant chambers are pulled off using a hydrogen torch. All the chambers are evacuated using a tube in the center reactor chamber. The reactants are kept hot (~ 300°C), and the pressure is lowered to a range of 1 to 5 x 10^{-4} Torr using a diffusion pump trapped with liquid nitrogen. The next step is to seal off the reaction chamber while the reduced pressure is maintained. After seal-off, the reactants are distilled through the frit into the center chamber. Care is taken to use temperatures that do not produce a vapor pressure above one mosphere. The temperatures for selenium and arsenic are 650 to 700°C, respectively. Distillation for antimony required a temperature of 1000°C and was extremely slow. The reaction chamber which is not heated during the distillation step serves as a cooled surface for condensation of the reactant vapors. When the distillation is complete, the side chambers (or chamber) are pulled off using the hydrogen torch without losing the reduced pressure.

The final step in the glass preparation (Figure 3) is to place the compounding chamber in a rocking furnace, heat slowly to the compounding temperature (700 to 800°C), and rock for periods of from 12 to 48 hours. The glass is quenched from a temperature of 575°C. The rocking action is maintained while

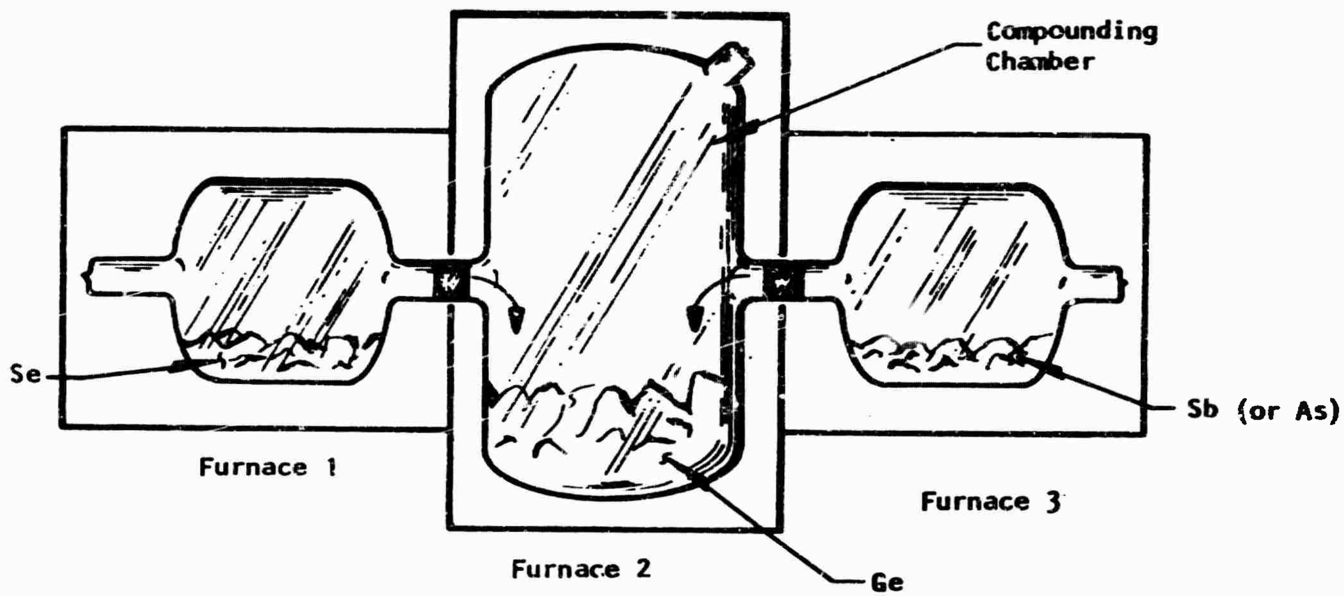

Figure 2 Distillation of Reactants Process Step

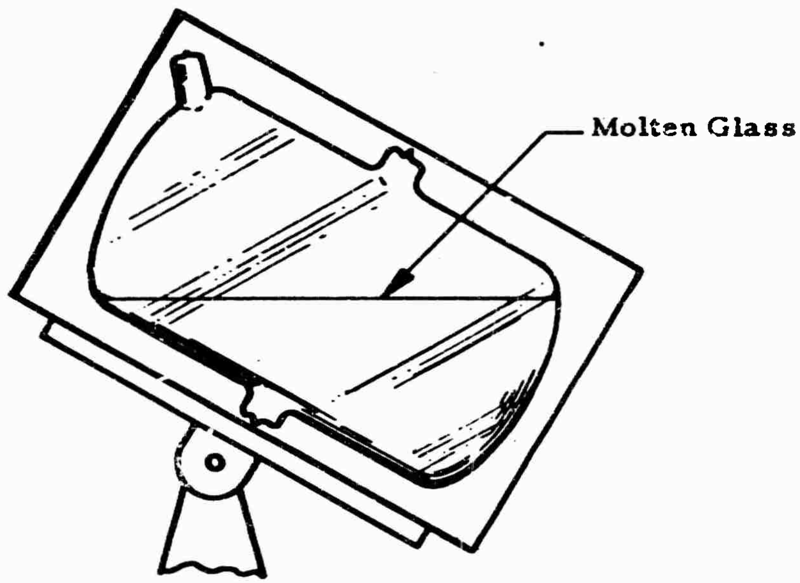

Figure 3 Apparatus Used for Glass Compounding

the molten glass is cooled to this temperature. Air-quenching is accomplished by turning off the power, opening the furnace (a split type), and blowing room air onto the quartz chamber using a hand-held blower. The furnace is placed in a near-upright position during this process to allow the melt to flow into the bottom of the chamber to provide a cylinder of glass. The process is continued until the glass sample and furnace elements reach an equilibrium temperature of 250 to 275°C. The furnace is then closed, and the glass is allowed to anneal at 275°C for six to eight hours. The final step is to cut off the power to the furnace and allow a slow cool-down for glass and furnace to room temperature. The entire operation for compounding 1 kgm of glass requires two to three weeks from start to finish.

C. Results

1. TI #1173

The first attempts to use the compounding methods described to prepare TI #1173 utilized the three-chamber method, but it was found that antimony distillation through a frit was impractical. The required amount of antimony (178 gm) was distilled at ~ 1000°C for about eight days, and no residue was left in the antimony container. It was therefore decided that in future preparation of the Ge-Sb-Se glass, only two chambers would be used, and the antimony would be placed in the center chamber along with the germanium. Both were treated for surface oxide removal at the same time. A trace amount of aluminum (~ 5 mgm) was added to the center chamber, as well.

The best results for TI #1173 prepared using the new methods and completely evaluated were obtained from run number 92. The calculated absorption coefficient as a function of wavelength is shown in Figure 4. The upper curve added to the diagram represents the expected absorption for good quality production-area cast TI #1173. Note that the magnitude of absorption at about 13 μm is 0.6 to 0.7 cm^{-1}, while it is 0.2 cm^{-1} for the 92 glass as a result of the addition of 5 ppm Al (none is added in the production area).

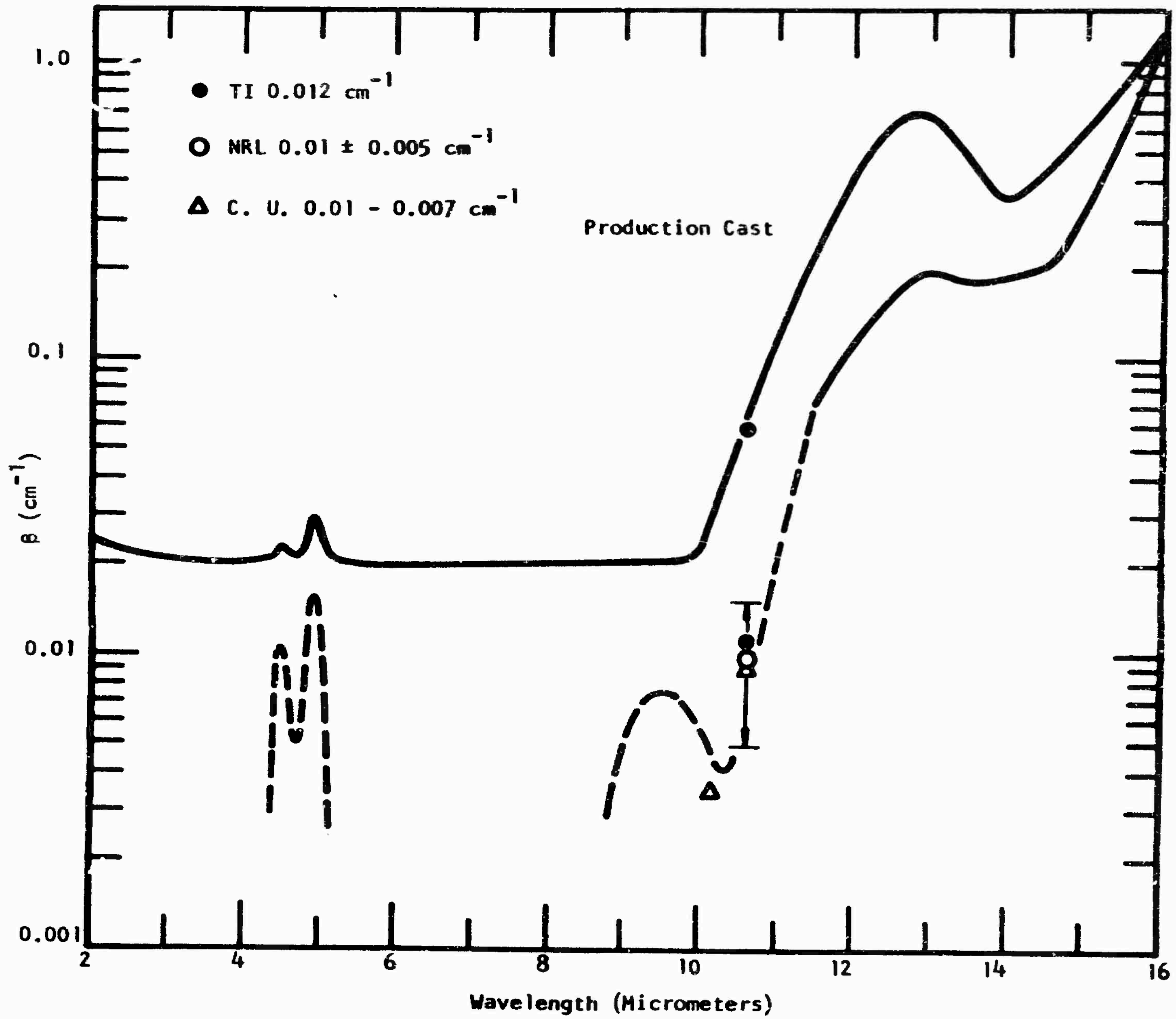

Figure 4 Absorption Coefficient as a Function of Wavelength for TI #1173

The measured laser calorimeter values have been added to the curves. TI #1173-92 was also evaluated by workers in other laboratories. The Naval Research Laboratory (NRL) value[13] at 10.6 μm was 0.01 ± 0.005 cm^{-1}. The Catholic University (C. U.) values[14] were 0.007 to 0.01 cm^{-1} at 10.6 μm and 0.0035 cm^{-1} at 10.15 μm. Our own value at 10.6 μm is 0.012 cm^{-1}, taken using the steady state method.

The dashed lines are values calculated using the expanded scale feature of the Perkin-Elmer 221. The method used is to estimate the increase in transmission from a point where a reasonably accurate value of the absorption coefficient can be calculated. The estimate is based on transmission measurements made with samples of two different thicknesses in an absorbing region. For these glasses the point was 11.5 μm using the Perkin-Elmer 337. The solid curve represents this determination. The dashed curve represents the estimated values from the Perkin-Elmer 221. As mentioned previously, the absorption-free transmission calculated using the precise refractive index measurements is an important means of verifying the validity of the values. Good agreement between laser calorimeter values and calculated values is obtained.

Two more features of the curve should be mentioned. First, a low-level absorption at ~ 9.4 μm is observed. After that absorption, the short wavelength region from 5 to 9 μm appears to reach the 0.001 to 0.002 cm^{-1} level. The two absorption peaks at 4.56 μm and at 4.95 μm presumably are due to dissolved gases. They are variable in magnitude and in intensity relative to one another. The two gases suspected of being the cause are H_2Se and H_2O. The magnitudes of the absorptions are again estimated by comparing 1X and 5X transmission scans. The presence of these two bands reflects the use of hydrogen during purification, perhaps the presence of residual dissolved gases in the reactants, and probably the evolution of H_2O from the quartz during the seal-off process.

The method produced low absorption glass. The next step would be to try to increase the purity further. Examination of previous reports and notebooks revealed that the only constituent that had not been varied relative to purity was germanium. Six-nines selenium and antimony had been used in this glass, as well as in previous batches in the production area, with no noticeable difference in absorption from glasses prepared with reactants of slightly lower purity. We decided to prepare glasses in which the known oxygen concentration was lower than the 0.2 to 0.3 ppm level of the first deposited germanium generally used. Also, single crystal germanium, because it had been melted in a reduced pressure environment, should contain a smaller amount of dissolved gases. Arrangements were made to purchase germanium with 30 ppb and 2.3 ppb oxide.[15] The design of the compounding apparatus was such that the germanium and antimony were placed in the compounding chamber without being broken to avoid exposure of the fresh surfaces to air. This required that a wide-mouth chamber be constructed and another chamber-end with a narrow pump-out tube sealed on the end after the reactants were added. To avoid hydrogen contamination, the oxide removal step was carried out while the reactants were heated under reduced pressure in both chambers. The distillation of selenium into the compounding chamber was carried out, the chamber sealed off, and the glass reacted in the usual manner. The glass compounded using the 30 ppb oxide germanium, TI #1173-107, yielded a laser calorimeter value of 0.019 cm^{-1} at 10.6 μm. Note that improvement is not observed. Also, the absorption at 9.4 μm and the gas absorptions at 4.54 μm and 4.96 μm increased. The level of absorption was barely below the 0.01 cm^{-1} value at 7 to 8 μm.

Results obtained with the 2.3 ppb oxide-containing germanium, TI #1173-109, were even worse. The laser calorimeter value at 10.6 μm was 0.024 cm^{-1}. The absorption at 9.4 μm has again increased while the two absorptions due to the dissolved gases have diminished. The general level of absorption for the glass was 0.01 to 0.02 cm^{-1} in the 5 to 8 μm range.

2. TI #20

The same procedure was followed for TI #20 glass except that the arsenic was placed in the same chamber as the selenium. Oxide removal was conducted at a little higher temperature (350°C) using hydrogen. The germanium was the semiconductor-grade germanium (0.2 to 3 ppm oxide) normally used, while the arsenic was the same six-nines pure material used in the production area for high purity GaAs. Complete distillation through the double frits required 700°C maximum temperature. The calculated absorption as a function of wavelength for TI #20-98 is shown in Figure 5. The top curve, added for comparison, represents results obtained from a piece of good quality, cast production area material. The 10.6 μm laser calorimeter values, 0.054 cm^{-1} for TI #20-98 and 0.057 cm^{-1} for production glass, have been added and agree well with the calculated results. The point to notice is that the magnitudes for both glasses are large relative to TI #1173. In addition, the production glass contains a peak around 8 μm which indicates the presence of a large amount of oxide. The magnitude of the 9.4 μm band is large for both glasses. Examination of the glass using the infrared microscope revealed that some of the particulate matter was not filtered out by the frit. The arsenic seems to be a major contributor. Also, condensation from the vapors above the glass falls into the melt, leaving particles in the glass that are transparent, but visible in the infrared microscope.

The synthesis of another batch, TI #20-102, was carried out using three chambers (to separate the arsenic from the selenium), but no better results were obtained. The Ge-As-Se glasses appear much more difficult to synthesize than the Ge-Sb-Se glasses. Examination of past reports and notebooks reveals that the absorption level has been consistently higher in these glasses than in the Ge-Sb-Se glasses, with the absorption coefficient of the order of 0.05 cm^{-1} even in the 6 to 8 μm region.

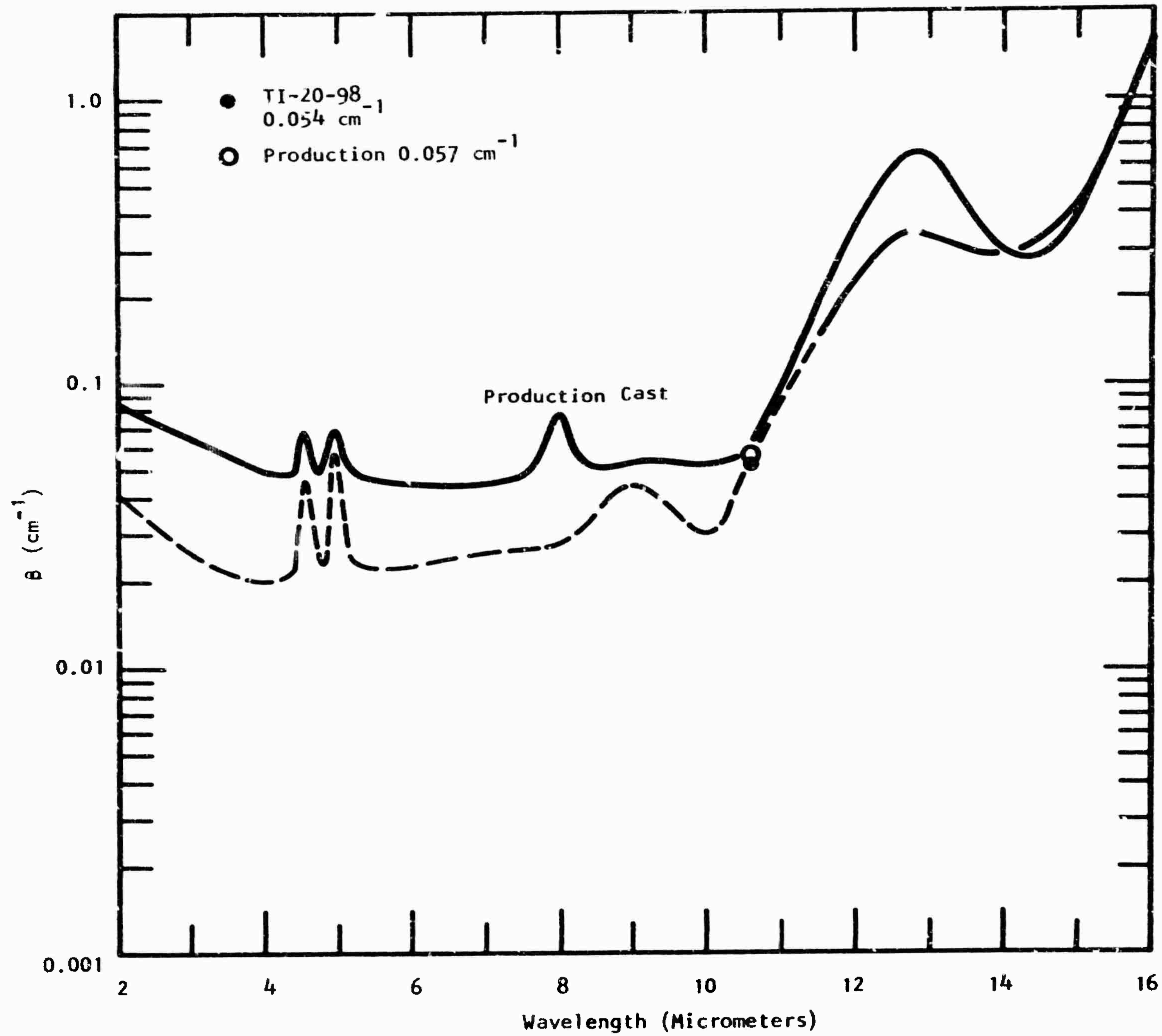

Figure 5 Absorption Coefficient as a Function of Wavelength for TI #20

3. Purity of the Glasses

a. Carbon

The as-received selenium residue left after distillation is amorphous carbon (according to x-ray analysis) in varying amounts. Measured carbon analyses have been in the 100 to 150 ppm range. It should be pointed out that the size and distribution of the carbon particles are variables that for glasses compounded without selenium distillation depend on reaction temperature, reaction time, physical agitation, and the beginning concentration of carbon in the selenium. However, examination of the compounded glasses before measurement with the laser calorimeter shows that essentially all the carbon is removed by the frits.

b. Emission Spectrographic Analysis

Results obtained from the analysis of TI #1173 and TI #20 samples prepared in this program consistently show the presence of Mg, Pb, Fe, and Cu in quantities from 0.1 to 1 ppm. These elements are commonly found contaminants in semiconductor materials prepared at high temperatures in high purity quartz. As metallic impurities, the elements pose no threat to the infrared transmission of the glass. Even if they were present as oxides, they would pose no real problem because their concentration is low and the reported occurrence for their major absorptions is at wavelengths beyond the 15 μm range of concern. The only impurity that appears to be affecting transmission in the region of interest is Si. The silicon is probably present as silica and gets into the glass from the area where the quartz containers are sealed off using the hydrogen torch. Table I presents a summary of the absorption data and important impurity results for the TI #1173 and TI #20 samples. Spectroscopically, the glasses are very pure. Impurities listed are the only ones found in concentrations of 1 ppm or greater.

Table I

Impurities and Absorption in TI #1173 and TI #20 Glass

Glass	[Si] ppm	[O] ppm ± 2	[Al] ppm	β 10.6 μm cm^{-1}	β ∼ 13 μm cm^{-1}	β ∼ 9.4 μm cm^{-1}
1173-P	2.5	4	0.3†	0.06	0.65†	---
1173-92	1.4	5.5	6.1	0.012	0.19	0.0075
1173-107	2.6	5.5	6.3	0.019	0.25	0.022
1173-109	2.2	4.5	6.1	0.024	0.25	0.025
1173-122	1.1	---	5.7	0.013	0.22	0.015
20-P	2.2	6	0.4†	0.056	0.65†	---
20-98	4.4	5	5.3	0.053	0.34	0.045
20-102	3.3	---	5.6	---	---	---
Ge	N.D.	8	N.D.	---	---	---
Sb	N.D.	---	N.D.	---	---	---
Se	N.D.	---	N.D.	---	---	---

†No Aluminum Added

N.D. - Not Detected

The [Si] and [Al] values are emission spectrograph results. The [O] values were obtained from the neutron activation procedure worked out at the Center for Trace Element Characterization at Texas A&M University. The reliability figure placed on the results is ± 2 ppm. The absorption values listed are the laser calorimeter value for 10.6 μm, the peak in the absorption around 13 μm obtained from IR transmission, and the absorption magnitude at around 9.4 μm obtained using the expanded-scale transmission measurement.

The first point to note is that no aluminum was deliberately added to the two production area glasses, TI #1173-P and TI #20-P; therefore, they had large absorptions at 10.6 μm and 13 μm. This fact is dramatically illustrated in Figure 6, which shows the measured transmission of TI #1173 about 1 cm thick with and without 5 ppm Al. The curve shows that the transmission at 10.6 μm is affected by the magnitude of the absorption at 12.8 μm. Almost identical curves have been reported in previous work at Texas Instruments[16] for TI #20 ($Ge_{33}As_{12}Se_{55}$) and for glass 56-8 ($Ge_{35}As_{15}Se_{50}$). The residual absorption that remains after addition of the Al is almost identical for all three glass compositions.

Large amounts of Al were found to produce no further change in absorption than did the 5 to 10 ppm quantities. Amounts up to 1000 ppm, even 1 to 2 atom %, were used. The larger quantities promoted an attack on the quartz container, as indicated by the appearance of "silicate" bands. Trace quantities of silver, magnesium, and potassium chloride were used with no apparent effect. However, zirconium and copper were found to be effective. With large amounts of copper (1 to 2 atom %), the transmission again had the same appearance one would obtain with 5 to 10 ppm Al.[16]

Table I shows that the oxygen concentrations for the production glasses and the ones prepared in this program are essentially the same. TI #20

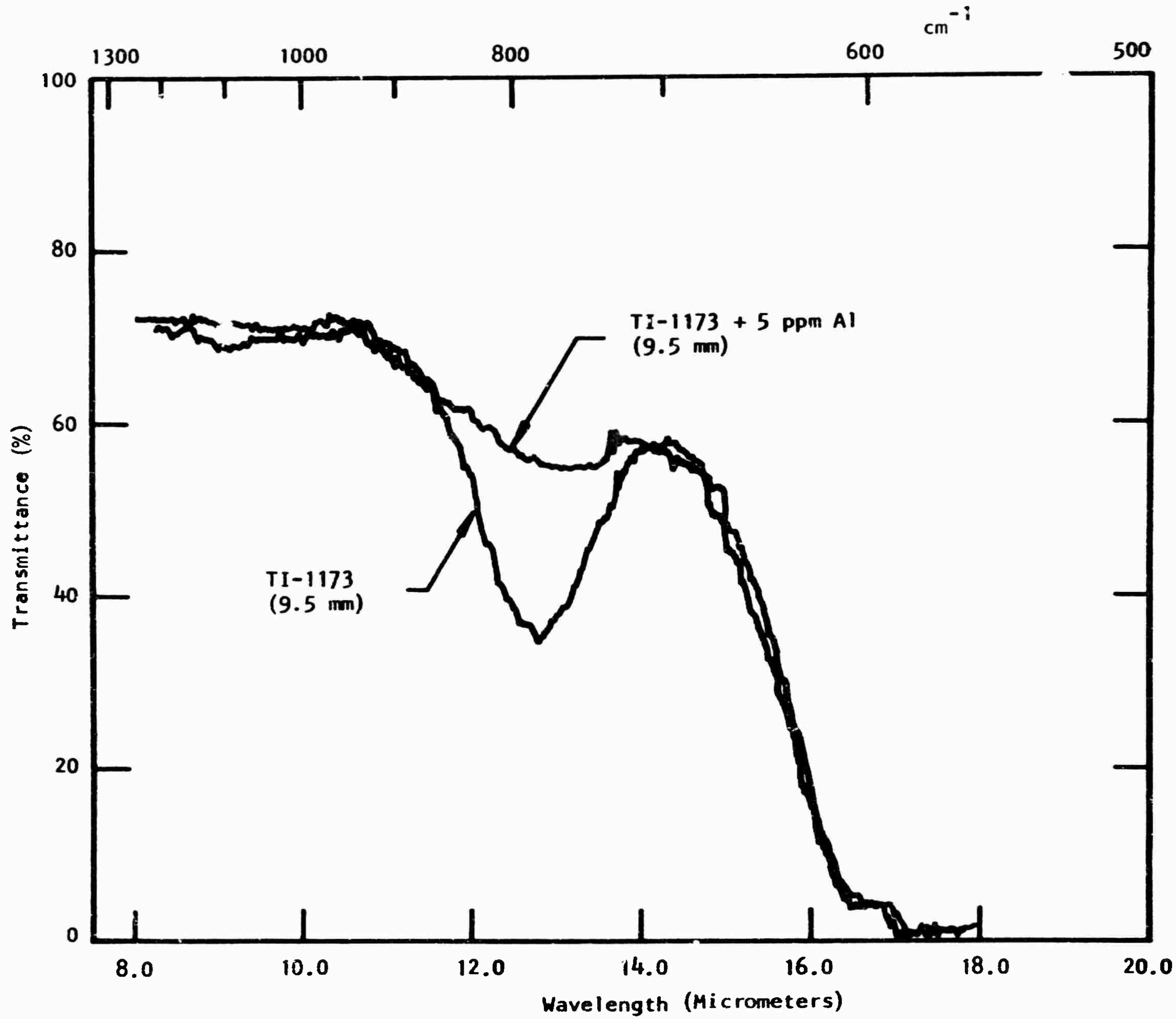

Figure 6 Effect of Trace Aluminum on the Infrared Transmission of TI #1173

seems to have a little more oxygen than TI #1173, but otherwise the values (within experimental accuracy) are the same. The indicated [O] in germanium concentration is surprisingly high compared to our infrared value, for reasons unexplained at this time. The most important factor is that the indicated oxygen concentration is almost identical to the aluminum concentration (5 ppm) found to be most effective in reducing the 12.8 μm absorption. This fact firmly supports the idea that the "gettering" action of the aluminum explains why a larger quantity of trace metal provides no further reduction in absorption. In reality, two absorption bands must be present, one at about 12.6 μm due to the presence of oxygen (presumably Ge-O) and a second always present which is broad, low in magnitude, and centered about 13.4 μm in the Ge-Sb-Se glasses and about 12.8 μm in Ge-As-Se glasses.

4. Discussion of Results for TI #1173 and TI #20

The only factor in Table I that shows any significant variation and correlation with the absorption in the glasses is the [Si] concentration. Note that Si was not detected in the reactants and probably gets into the glass during the sealing procedure. Probably, silicon-oxygen containing molecules are liberated from the inner surface of the quartz container when the softening point (1400°C) is reached. The reactants become coated by a film of such a material. For this reason, our attempts to prepare glass with increased purity using the unbroken pieces of the low-oxygen germanium were thwarted by the increased exposure to silica brought about when the wide-mouth reaction chamber was sealed. To test this hypothesis, we synthesized another 1 kgm batch of TI #1173 using high purity reactants, hydrogen flow during oxide removal, and a reaction chamber designed to minimize the exposure of the ingredients to the silica produced during seal-off. The analytical results obtained are listed in Table I under run number 122. Notice the [Si] level is the lowest listed, and the laser calorimeter value is back in the 0.01 cm^{-1} range. Gas absorption in the 5 μm region is very high,

indicating the dissolved H_2 was not removed during seal-off. The 9.4 μm absorption level is of the order of 0.015 cm^{-1}.

A plot of the [Si] for the four TI #1173 samples as a function of the measured 10.6 μm absorption coefficient is shown in Figure 7. The only comparable value for TI #20 is shown as a (+) on the diagram. From all the information present, it appears that the absorption at 10.6 μm in TI #1173 at this degree of purity is dominated by the [Si], present probably in the form of silica. The absorption band at 9.4 μm occurs where the Si-O stretch generally is found, as in the case of silicon. A better correlation between the 9.4 μm absorption and silicon content is shown in Figure 8. Again, the TI #20-98 value has been added, showing a direct correlation as well.

Examination of Figure 4 and Figure 5 shows that the 9.4 μm absorption adds onto the absorption that occurs around 13 μm in both the Ge-Sb-Se and Ge-As-Se glasses. For the Ge-Sb-Se glass, the absorption center occurs at a wavelength slightly longer than 13 μm. Therefore, the domination of the 10.6 μm value is not as pronounced, and lowering the 9.4 μm level should lead to a lower 10.6 μm level. For the Ge-As-Se glass, the broad absorption is centered at a wavelength slightly less than 13 μm. The 10.6 μm value is dominated by that band more severely than the 9.4 μm band. Lowering the silica content will improve the 10.6 μm value only slightly.

5. Origin of the Absorption at ~ 13 μm in Ge-Sb-Se and Ge-As-Se Glasses

Lucovsky, et al.,[17] at Xerox and Twaddel, et al.,[18] at UCLA have indicated that the IR absorption at 13.4 μm (744 cm^{-1}) in amorphous selenium is due to the presence of Se_8 rings. Twaddel, et al.,[18] stated that the absorption could be made to disappear in a reaction catalyzed by the potassium ion. The Xerox work[17] showed that the band disappeared when arsenic was added to selenium,

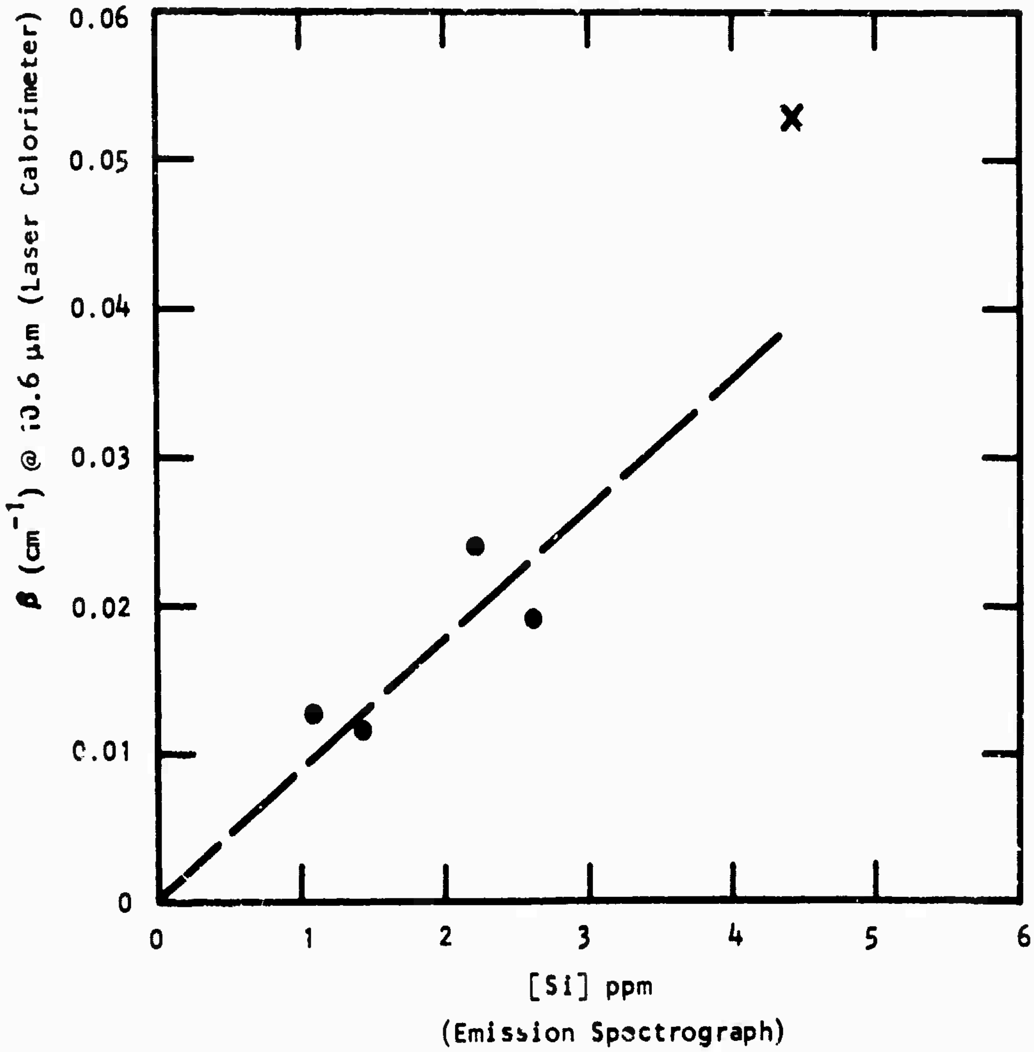

Figure 7 Absorption at 10.6 μm in TI #1173 and TI #20 as a Function of Silicon Content

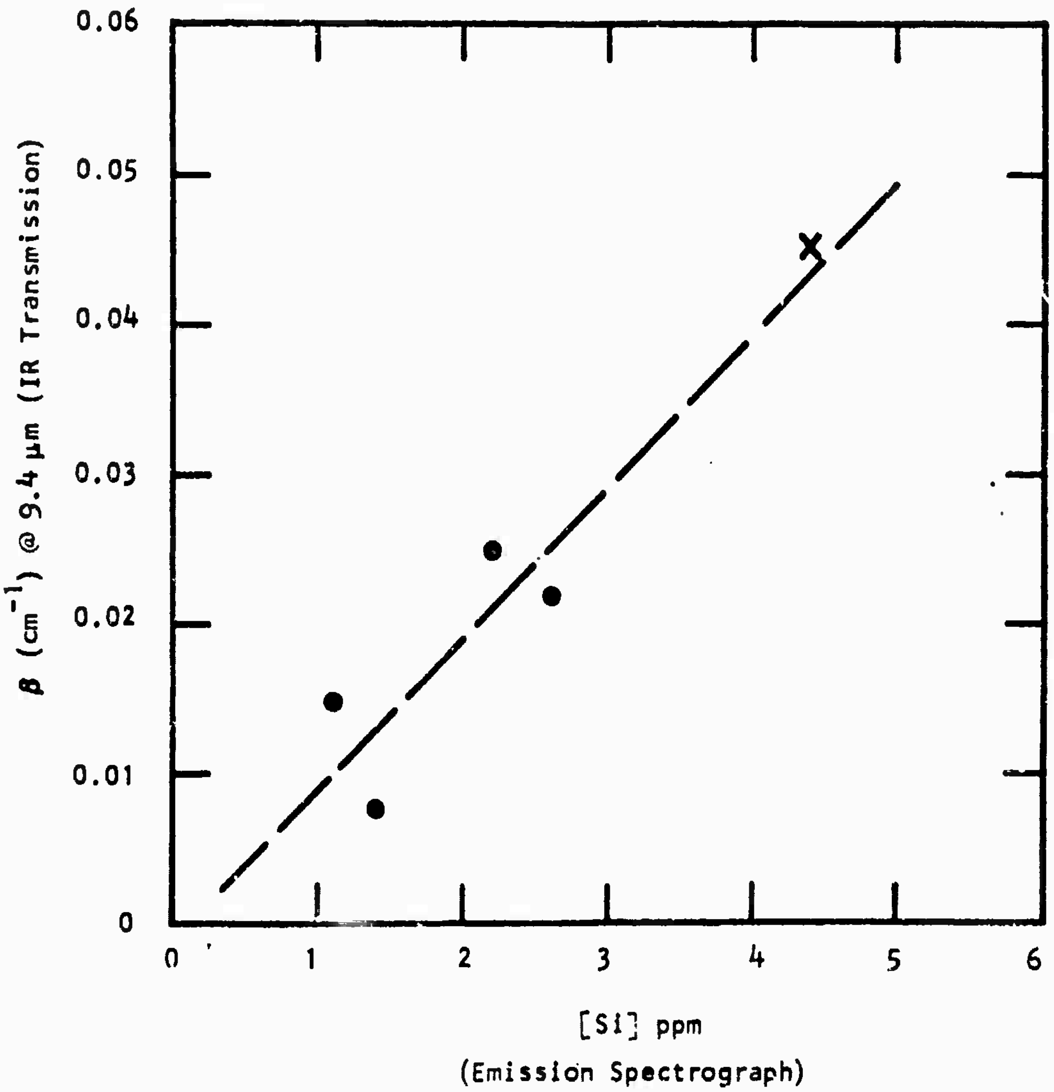

Figure 8 Correlation Between Absorption at 9.4 μm and Silicon Content in TI #1173 and TI #20

and a new band characteristic of As-Se appeared. Results obtained in our own laboratory indicated that the 13.4 μm band did not disappear when germanium was added, but merely shifted to shorter wavelength (12.8 μm). Our results appeared to agree with and substantiate the Xerox conclusion[17] that in their experiments As was introduced into the Se_8 rings. For Ge-As-Se and Ge-Sb-Se glasses, the introduction of the elements into the ring shifted the frequency of the absorption and increased its magnitude. We speculated[8] then that the effect of small amounts of Al, Zr, etc., might be a catalyzed decomposition of the ring structure. However, in view of the results reported in the previous section, it appears the effect observed was due primarily to removal of the oxide absorption centered around 12.6 μm. In fact, when As or Ge was added to amorphous Se, the oxide that was introduced produced a band that far overshadowed the broad, low level absorption centered around 13 μm in the Ge-Sb-Se and Ge-As-Se glasses.

The temperature dependence of the absorptions in the glasses is very important in helping to understand the origin of each. Absorptions arising from isolated impurities usually exhibit only weak temperature dependence, while intrinsic absorptions due to vibrational, electronic, or magnetic excitations generally show strong changes with temperature. To illustrate these statements, the transmittance of TI #1173 without the addition of Al and with the addition of Al measured between room temperature and 77 K is shown in Figures 9(a) and 9(b). The measurements were performed using the Perkin-Elmer E-1 system. Only small changes occur until a wavelength of 12.5 μm is reached for both glasses. This fact is illustrated by plotting the difference (77 K to room temperature) at the bottom of the curve showing the wavelength location of the thermally sensitive absorptions. In Figure 9(b), we find that the remaining absorption centered around 13.4 μm is reduced in magnitude and shifted toward shorter wavelength. The broad band in Figure 9(a) shifts to 12.7 μm, indicating the impurity band is centered more nearly at 12.6 μm. Combining the two bands still leads to a peak

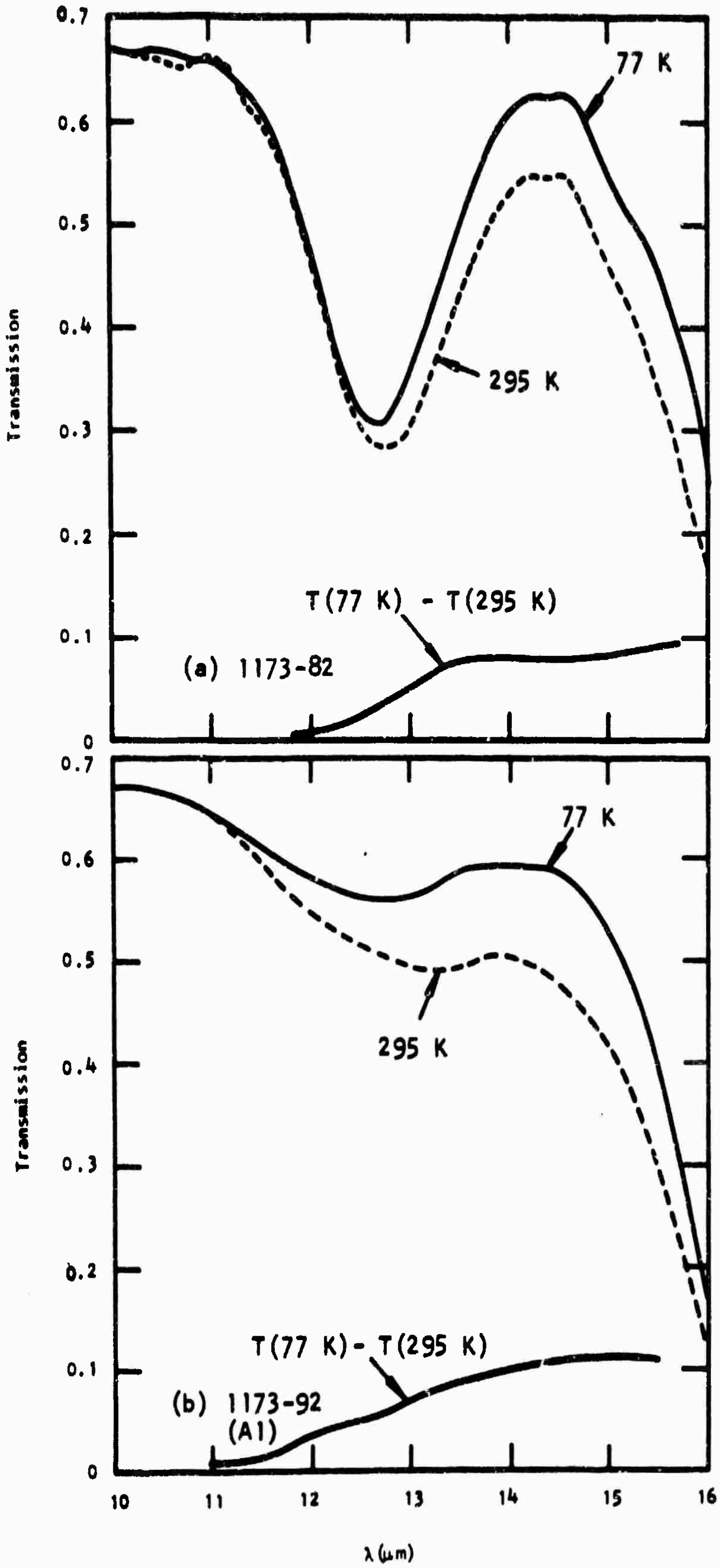

Figure 9 Transmission of TI #1173 With and Without Aluminum as a Function of Temperature

at 12.8 μm. Prior to the successful preparation of high purity gettered TI #1173 glass, the strong oxide absorption at 12.6 μm obscured the thermally active absorption in this spectral region. To learn more about the thermally active character of this band, the measurements were extended to higher temperatures over the wavelength range out to 18 μm. The results covering -196°C to +207°C are shown in Figure 10. The temperature dependence is quite strong, particularly for temperatures in excess of ambient. Assuming the absorption peak varies in a power law manner, $\alpha \sim T^x$, the absorption coefficient at 13 μm was found to have the value of $x = 1.85 \pm 0.15$, within the predicted temperature dependence for a third order multiphonon excitation. However, there is some discrepancy in the wavelength location of the peaks. From IR reflection spectra obtained in our laboratory, the strongest absorption is estimated to occur at 235 cm^{-1}, with an absorption maxima estimated to be 7500 cm^{-1}. A confirmation of the resonance frequency is found in the Raman data reported to us[13] by Dr. Marvin Hass of NRL. Dr. Hass reported two frequencies for $Ge_{28}Sb_{12}Se_{60}$: 230 cm^{-1} and 193 cm^{-1}. Doubling and tripling our 235 cm^{-1} value leads to 470 cm^{-1} and 705 cm^{-1}, in contrast to the observed values of 490 cm^{-1}, 560 cm^{-1}, and 745 cm^{-1}. Assuming ωf = 235 cm^{-1}, a $\omega/\omega f$ plot for TI #1173 is shown in Figure 11 for room temperature and liquid nitrogen data. The slopes for an exponential decay from the β_o = 7500 cm^{-1} of $\beta \sim \beta^{-2\omega/\omega f}$ and $\beta \sim \beta^{-3\omega/\omega f}$ are shown as dashed lines for reference. Note that the dependence for the peaks in absorption, below room temperature, is slight.

Considering all the evidence presented above, it appears very likely that the broad intrinsic absorption that occurs at slightly less than 13 μm in TI #20 and slightly more than 13 μm in TI #1173 is due to a third order stretching vibration between Ge and Se atoms. The coupling of the heavy antimony atoms tends to shift the vibrations to lower frequency, while the arsenic atoms in TI #20 are about the same mass as germanium, leading to a higher frequency vibration. The configuration involved is probably a germanium atom surrounded by four selenium atoms in a tetrahedron.

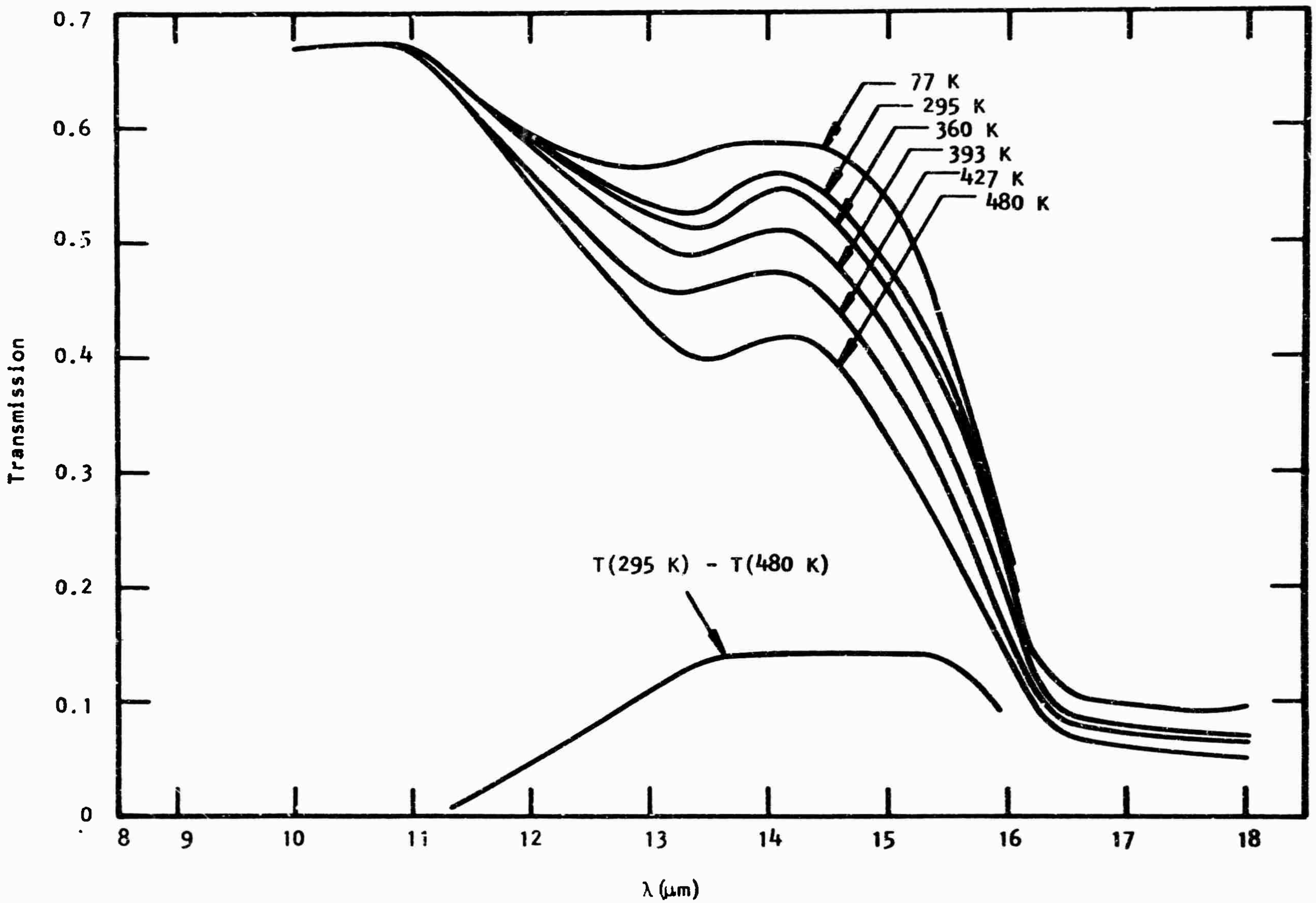

Figure 10 Transmission Above and Below Room Temperature of TI #1173 Treated With Trace Aluminum

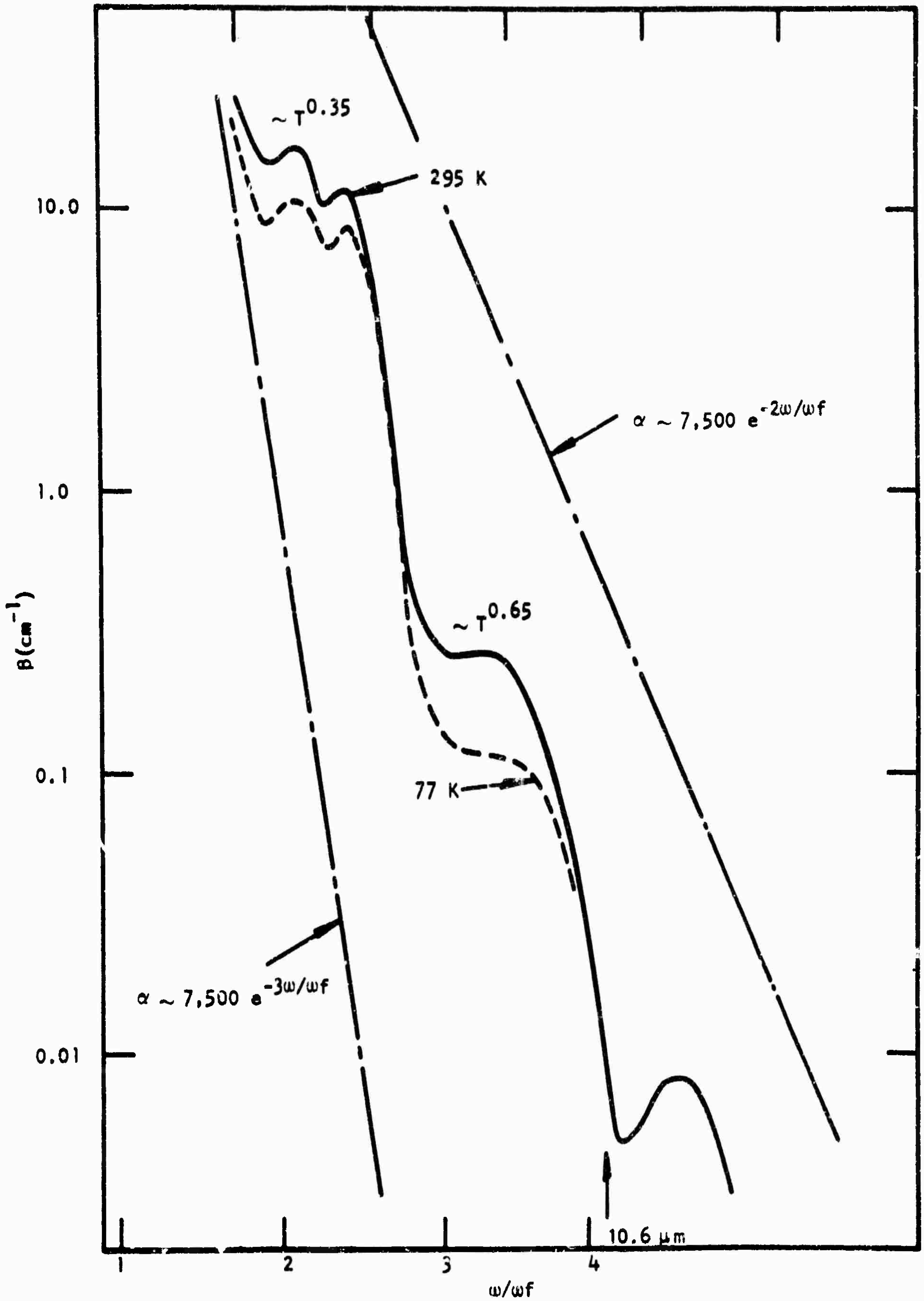

Figure 11 A Plot of Absorption as a Function of $\omega/\omega f$ for TI #1173 at 77 K and 295 K

The final illustration for TI #1173 describes the present condition of the absorption at the band edge. Results obtained in our laboratory are shown in Figure 12. The work of Tauc and Menth[19] has been added for reference. Their values are found to be more than one order of magnitude above our own. However, we know nothing of the quality of the $Ge_{28}Sb_{12}Se_{60}$ glass on which their measurements are based. The lowest curve represents the results obtained in another program in our laboratory[20] and is based on near-IR laser calorimeter values. The upper curve was obtained strictly from transmission measurements using a conventional spectrophotometer. The exponential absorption edge extrapolation to 10.6 μm indicates the level of absorption is not presently limited by the fundamental electronic absorption process.

D. <u>Conclusions</u>

1. The magnitude of the absorption coefficient at 10.6 μm in the Ge-Sb-Se glass TI #1173 at the present state of purity is about 0.01 cm^{-1}. The value is limited by the concentration of "silica" in the glass. Removal of this impurity and the associated absorption should reduce the magnitude of the absorption coefficient to the 0.001 to 0.005 cm^{-1} range. The absorption at 10.6 μm below this range is determined by a broad, low-level absorption (0.2 cm^{-1}) centered about 13.4 μm. The absorption appears to be intrinsic.

2. The magnitude of the absorption at 10.6 μm in the Ge-As-Se glass TI #20 at the present state of purity is about 0.05 cm^{-1}. The value is limited by a broad, low-level absorption (0.35 cm^{-1}) centered about 12.8 μm. The absorption appears to be intrinsic.

3. The broad, low-level absorption occurring around 13 μm in Ge-Sb-Se and Ge-As-Se glasses shows a temperature dependence for absorption that indicates a third order process. The origin of the band is probably the third order stretching vibration of a germanium atom surrounded by four selenium atoms in a tetrahedral configuration.

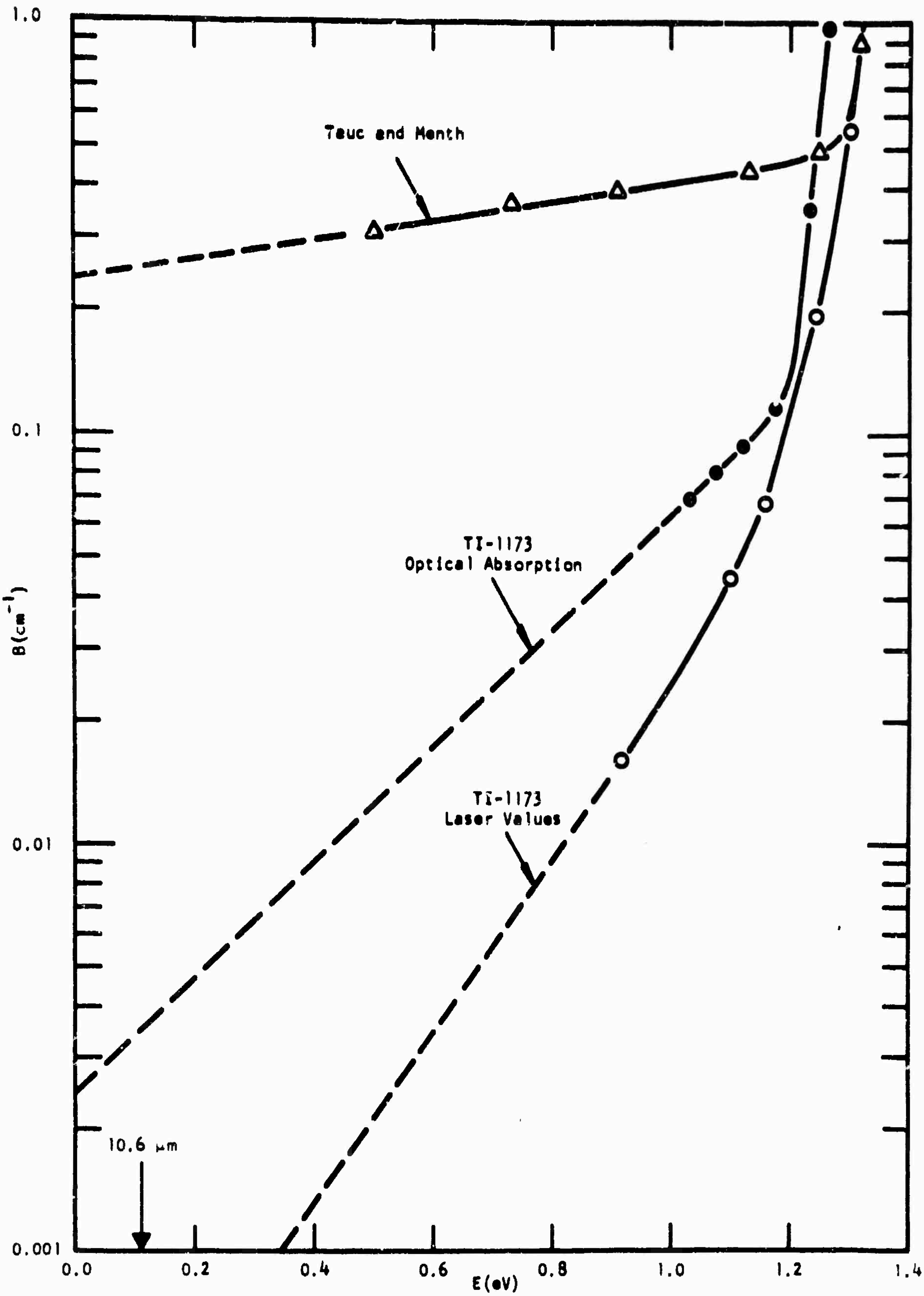

Figure 12 The Absorption Edge of TI #1173

SECTION III

THE INTERDEPENDENCE OF PHYSICAL PARAMETERS FOR INFRARED TRANSMITTING GLASSES

A. Evaluation of Physical Parameters

Physical parameters that will be discussed are density, glass transition temperature, volume expansion, hardness, thermal conductivity, elastic moduli, and Poisson's ratio. The evaluation methods are described below.

1. Density

The density was determined by the Archimedean method using an Ainsworth Analytical balance and distilled water as a medium. Density is important in the calculation of other parameters such as estimating the refractive index.[8]

2. Thermal Expansion and T_g

A quartz tube dilatometer was used to obtain both the coefficient of thermal expansion ($\Delta L/L$) and the glass transition temperature (T_g). The equipment was a Daytronic Model 300D Transducer Amplifier-Indicator with a Type 71 plug-in unit in conjunction with a Daytronic Linear displacement transducer. The system was capable of operating from room temperature to approximately 1000°C. A typical curve taken on an X-Y recorder is shown in Figure 13. The method used to define T_g is indicated in this figure. The differential thermal analysis method (DTA) was not used because residual strain in polished glass samples was found to significantly affect the results.

The glass transition temperature reflects the upper use temperature of the glass. The volume expansion term is important in the calculation of thermal lensing effects.[5,7]

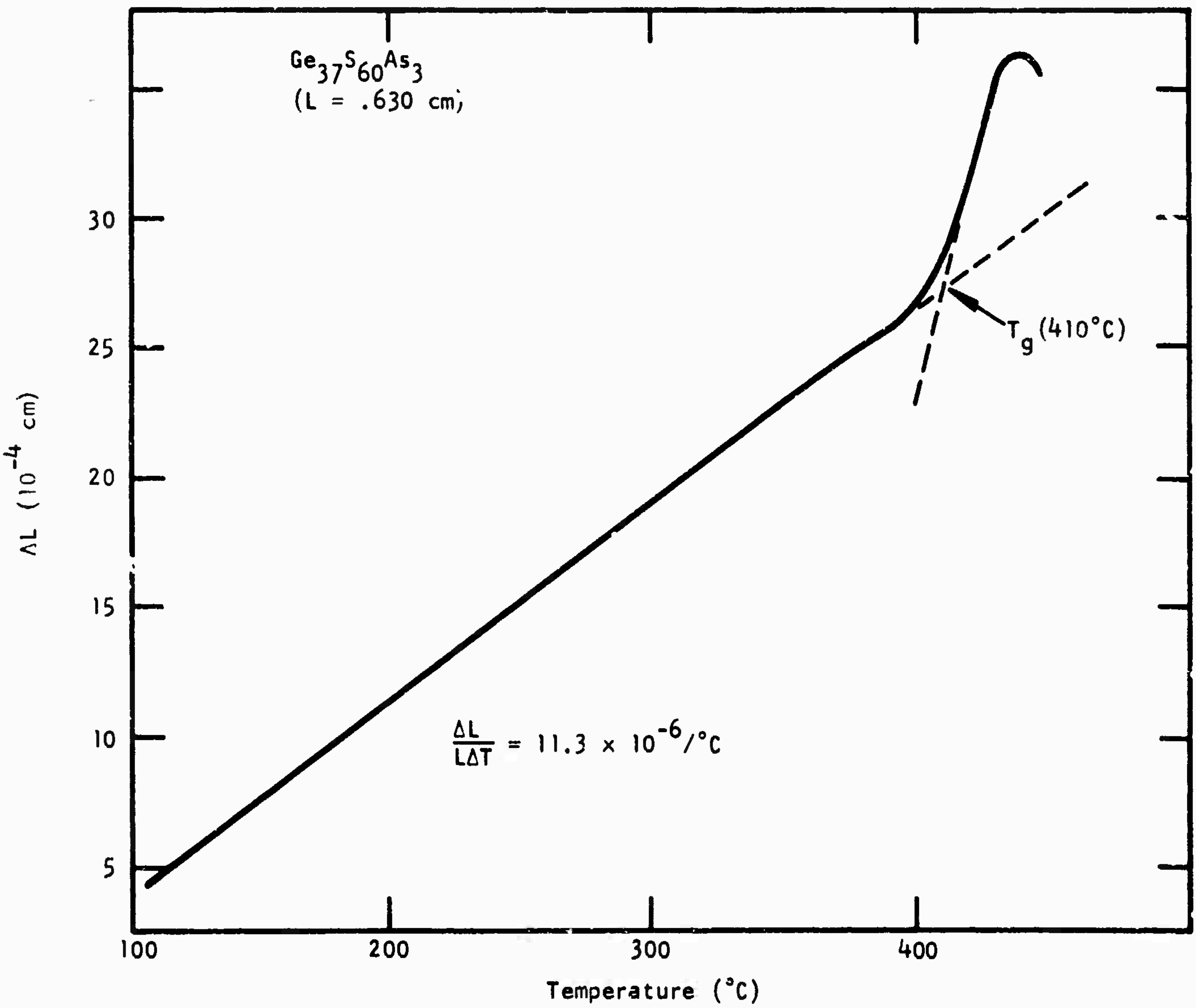

Figure 13 Dilatometer Measurement of Glass Transition Temperature

3. Hardness

Microhardness was measured using a Leitz Miniload Hardness Tester with a Knoop diamond. A small decrease in the hardness value is observed with increasing load when these relatively soft glasses are tested. For this reason, it is important to state the load used when reporting the hardness value. A 50 gm load was used during this study. Generally, hardness is found to be low for materials transparent at 10.6 μm.

4. Thermal Conductivity

The thermal conductivity of the sulfur- and selenium-based glasses was measured using a Thermal Comparator Model 100 obtained from McClure Park Corporation. This instrument works on the principle that the rate of cooling experienced by the tip of a heated probe upon contact with the surface of the sample can be related to the thermal conductivity when the system has been calibrated with known thermal conductivity standards. The quoted reproducibility is ± 2% or better, and the quoted accuracy is given as ± 5% or better on well-characterized surfaces.

Low thermal conductivity is, of course, an inherent limitation of IR glasses when faced with the high energy densities of CO_2 lasers. Removal of the absorbed heat is extremely slow, leading to thermal lensing.[5,21]

5. Elastic Moduli

The Young modulus (E) and the shear modulus (G) were determined on a series of selenium-based and sulfur-based glasses by measuring the velocity of both longitudinal (v_L) and shear (v_S) sound waves. Knowing these velocities and the density (ρ) of the material, E and G were calculated from the following relations:

$$E = 2G\,(1 + \nu), \quad G = \rho\, \nu_S^{\,2},$$

where Poisson's ratio (ν) is given by:

$$\nu = \tfrac{1}{2} - \tfrac{1}{2}\, \frac{\nu_S^{\,2}}{\nu_L^{\,2} - \nu_L^{\,2}} .$$

The sound velocities were measured by the pulse-echo method using a Sperry Attenuation Comparator with a 0 to 100 μsec digital delay. The absolute accuracy of such a system is slightly better than 1% for the velocity measurements. This would give approximately 2% accuracy in G and slightly less than this for E.

The elastic moduli are important in the calculation of other parameters. The resultant Poisson's ratio illustrates the transition within a glass-forming composition region from almost polymeric amorphous material in the high chalcogen region to a network type structure when the chalcogen falls below 60 atom %.

B. Interdependence of Physical Parameters

1. Density

Published results from this laboratory[22] for selenium- and tellurium-based glasses demonstrated a linear relationship between the calculated molecular weight for a glass composition and its density. At the time, very little data were available for sulfur-based glasses. The data available for As_2S_3 and S indicated that sulfur-based materials would lie on a line of slope different from that of selenium- or tellurium-based glasses. During this contract, several sulfur-based glasses were made available to us by workers on another glass program.[23] Addition of these points confirms the earlier speculation. Figure 14 shows a plot of measured density as a function of molecular weight for sulfur- and selenium-based glasses. Two separate slopes are obtained, with a mixed S-Se glass in between.

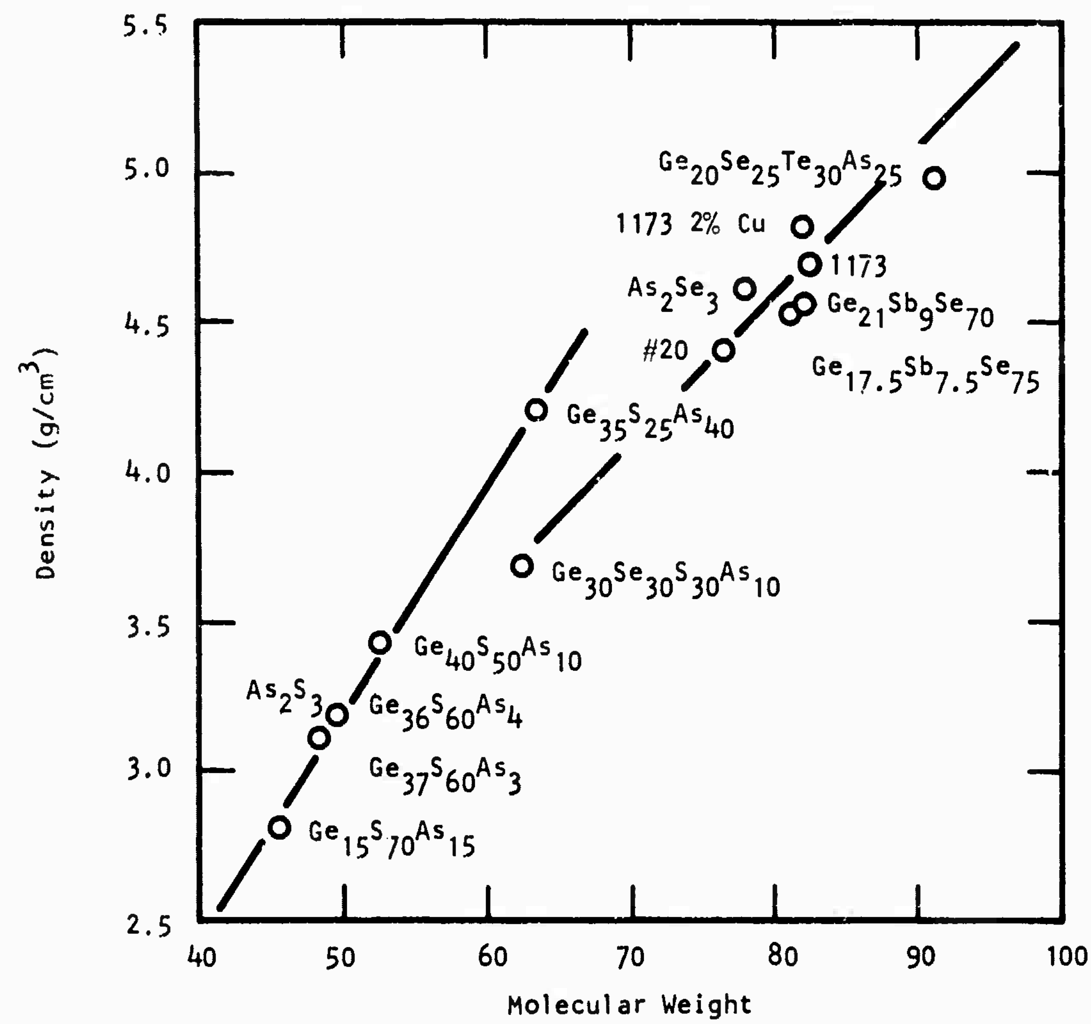

Figure 14 Density as a Function of Molecular Weight for Some Selenium and Sulfur Glasses

2. Thermal Expansion and T_g

A review article by Gschneider[24] pointed out that for over 85 years investigators have noted that crystalline materials with high melting points have low coefficients of thermal expansion, and vice versa. Sakka and Mackenzie[25] pointed out recently that a simple empirical rule,

$$T_g/T_m = 2/3,$$

where T_g is the glass transition temperature and T_m is the crystalline melting point, holds surprisingly well for inorganic systems. Putting these two observations together, one would expect glasses with high T_g to have low coefficients of expansion. The measured values for many glass compositions are shown in Figure 15. The general trend is apparent, but there is considerable variation among glasses of widely different composition. Since T_g should reflect the weaker, long-range forces in a multicomponent system, it should not be surprising to see some compositions vary widely from expected behavior. For example, the points for 1%, 2% Cu in TI #1173 and the point for 1% Al in TI #1173 show both T_g and the volume expansion decreasing from the values for pure TI #1173. With a decrease in volume expansion, one would expect T_g to increase. An explanation for this apparent discrepancy is that the addition of Cu or Al leads to the formation of small molecules which fit into the void spaces in the network structure. Thus, the long-range forces between the network units are weakened.

3. Elastic Moduli

Table II lists the Young's modulus and the shear modulus as determined from sound velocity measurements for several glass compositions. The calculated Poisson's ratio for each composition is given in the third column. A second value for TI #20 taken from the literature[26] is shown for comparison to indicate the accuracy and reproducibility of the method.

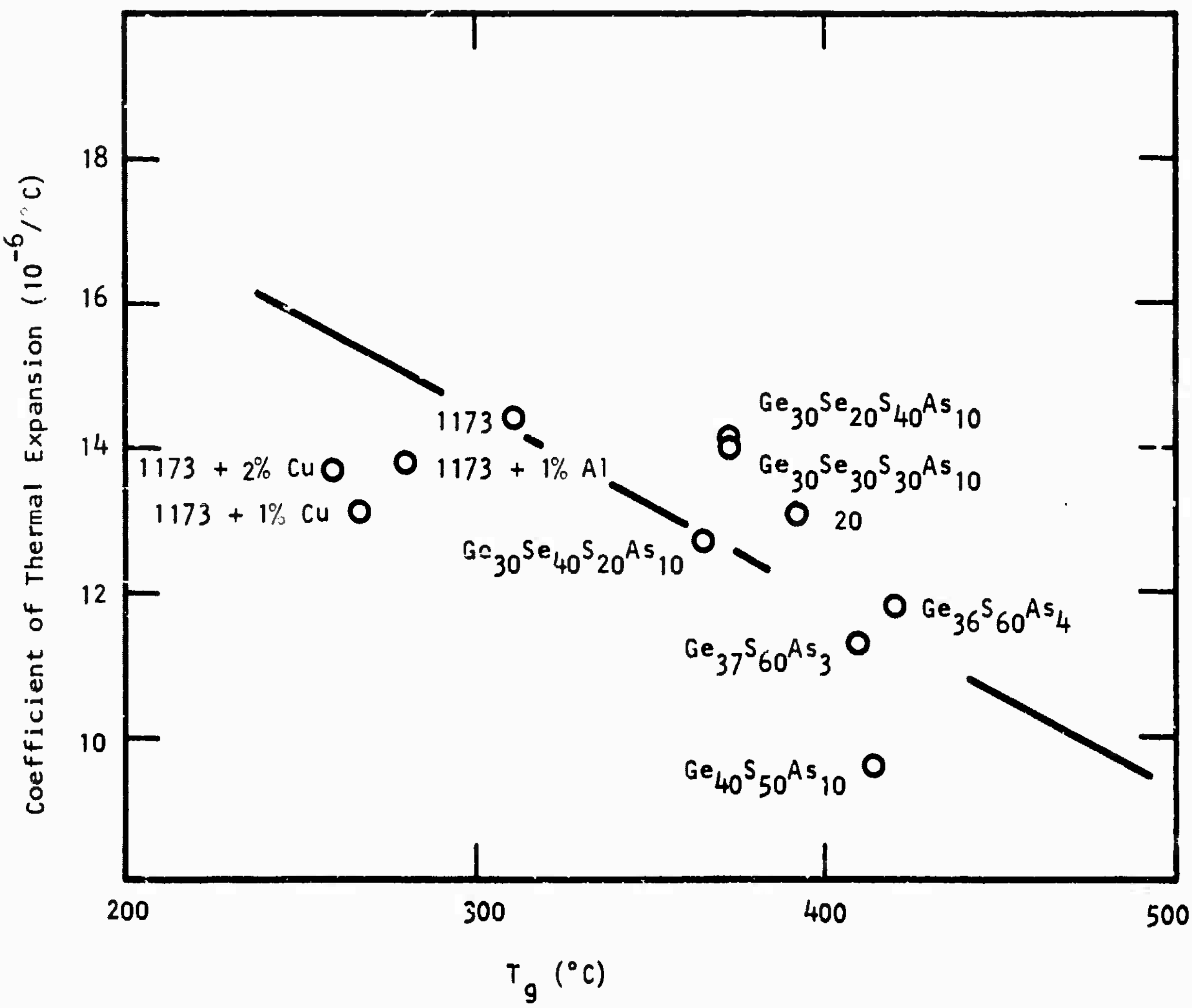

Figure 15 Thermal Expansion Coefficient and Glass Transition Temperature (T_g) for Some Sulfur and Selenium Glasses

Table II

Elastic Moduli of Sulfur- and Selenium-Based Glasses

	E (10^6 psi)	G (10^6 psi)	ν
Se	1.43	0.545	0.315
$Ge_{17.5}Sb_{7.5}Se_{75}$	2.35	0.92	0.279
$Ge_{21}Sb_{9}Se_{70}$	2.56	1.00	0.278
$Ge_{28}Sb_{12}Se_{60}$ (1173)	3.16	1.26	0.265
As_2Se_3	2.65	1.03	0.289
#20	3.17	1.26	0.266
#20 (Bell Labs[12])	3.29	1.31	0.261
$Ge_{15}S_{70}As_{15}$	2.01	0.776	0.295
$Ge_{36}S_{60}As_{4}$	3.05	1.22	0.250
$Ge_{37}S_{60}As_{3}$	3.37	1.38	0.244
$Ge_{40}S_{50}As_{10}$	4.26	1.70	0.251
$Ge_{35}S_{25}As_{40}$	6.08	2.39	0.271
$Ge_{30}Se_{30}S_{30}As_{10}$	2.72	1.02	0.274
$Ge_{20}Se_{25}Te_{30}As_{25}$	3.00	1.18	0.270

Note the decrease in Poisson's ratio as composition is changed from glassy selenium toward the network structure glass TI #1173. The value decreases, indicating a change from polymeric to network form. The other two glasses listed in the series have the same Ge/Sb ratio as $Ge_{28}Sb_{12}Se_{60}$, TI #1173. Even lower values of Poisson's ratio are noted for sulfur-based glasses that are high in Ge and As, but low in sulfur. Increases in elastic moduli of 2 to 4 times the selenium value are found for sulfur-based materials.

4. Hardness

A straight-line relationship between the measured hardness and Young's modulus is found for the selenium- and sulfur-based glasses shown in Figure 16. The slopes for the two families of glasses are different, reflecting to some extent the relative strengths of the primary bonds formed between the metallic elements and the sulfur or selenium atoms. However, there is the other factor, density, in Young's modulus to consider. Variation around the sulfur glass or selenium glass hardness vs Young's modulus line can be expected, depending on the atomic masses of the group IVA and VA elements in a ternary system. For example, in Figure 4 results are presented for the Ge-As-S glasses where the atomic masses of the elements germanium and arsenic are almost the same. Good correlation can be expected. However, the correlation should not be as good when the IVA and VA elements are germanium and antimony. Here, the atomic masses are quite different, which introduces a density factor as the IVA/VA ratio changes.

5. Thermal Conductivity

The room temperature values of thermal conductivity for 14 chalcogenide glasses of different compositions were obtained using the Thermal Comparator. These values are plotted as a function of their respective longitudinal sound velocities (also measured at room temperature) in Figure 17. An excellent linear correlation is observed.

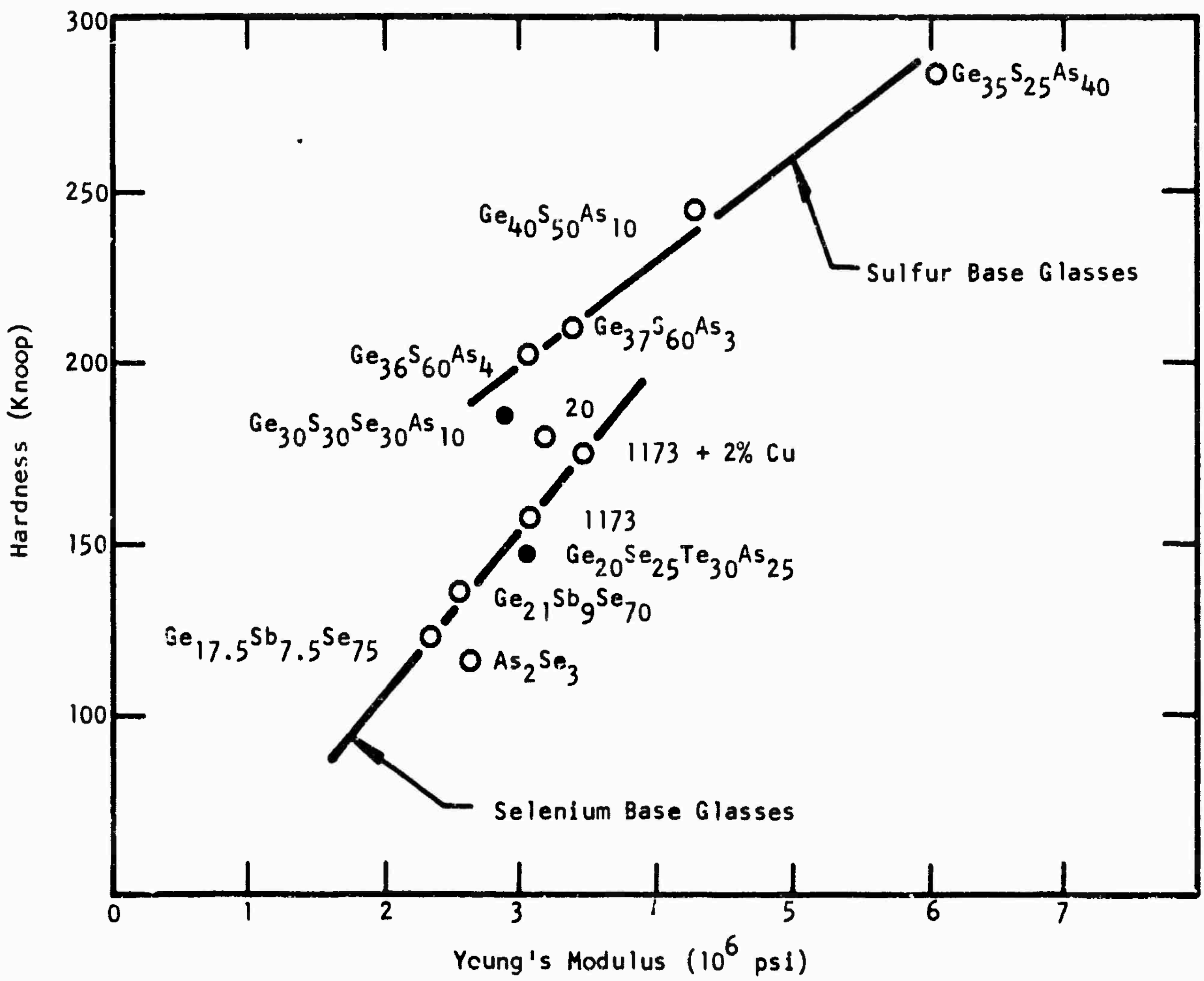

Figure 16 Hardness vs Young's Modulus for Sulfur and Selenium Glasses

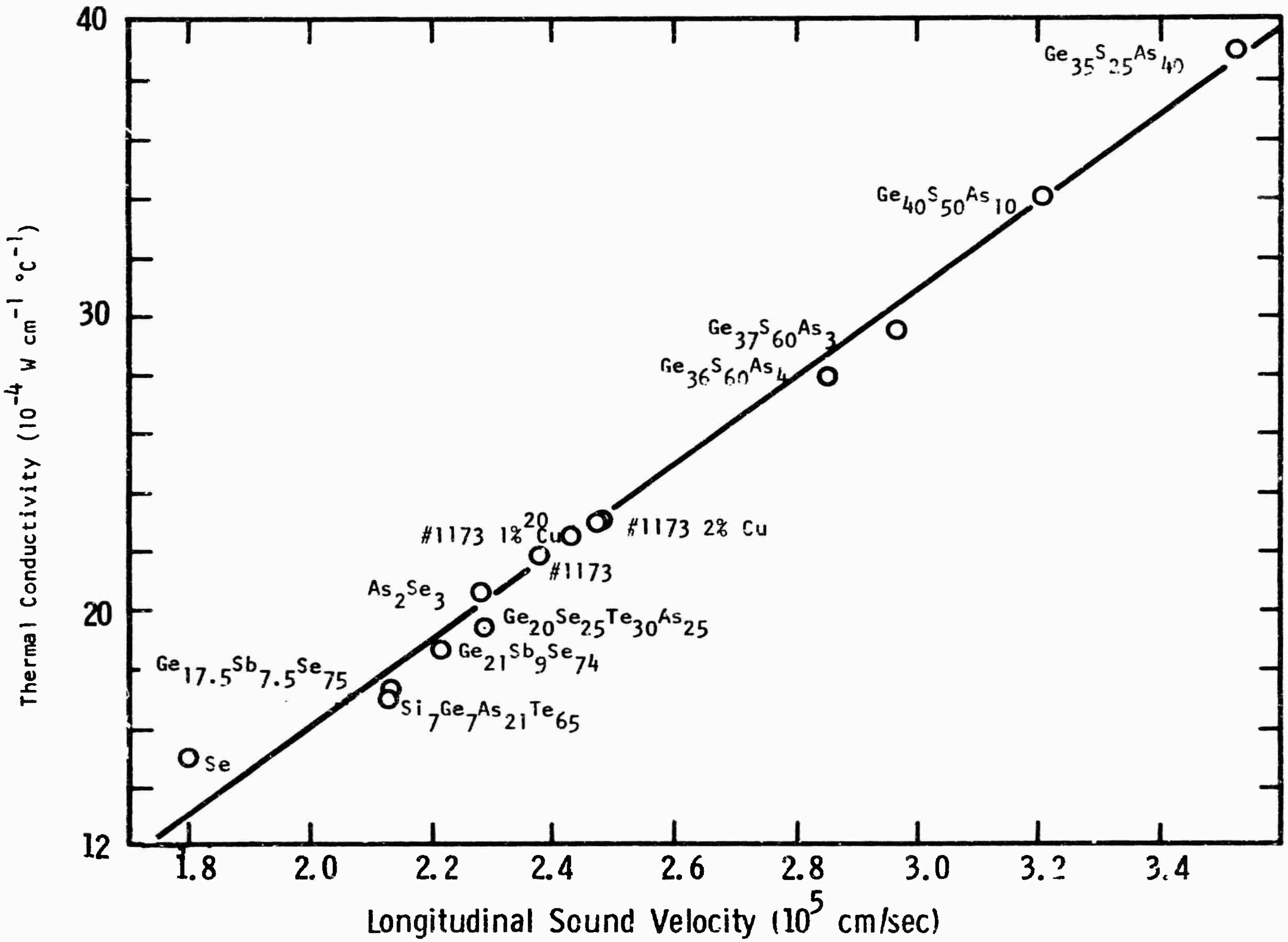

Figure 17 Thermal Conductivity vs Longitudinal Sound Velocity for Some Sulfur and Selenium Glasses

Stourac, et al.,[27] reported in 1968 the measured thermal conductivities for a series of Ge-Se glasses. The observed increase in thermal conductivity with increasing germanium content was explained as being related to the observed increase in sound velocity. The results of Stourac, et al.,[27] and our own linear relationship may be explained by applying the simple Debye expression for thermal conductivity due to phonons:

$$K = \frac{1}{3} C_V V \bar{\ell} ,$$

where C_V is the heat capacity per unit volume,

V is the average phonon velocity (related to the sound velocity), and

$\bar{\ell}$ is the mean free path for phonons.

Workers at Catholic University pointed out[28] that the heat capacity values for TI #1173 and TI #20 reach almost their maximum values (3R) by room temperature. For chalcogenide glasses with low Debye temperatures, C_V would be expected to vary only slightly with composition. The value of $\bar{\ell}$ is a measure of the disorder (or lack of three-dimensional order) for the melt-formed glasses and should change very little with composition. The only remaining function, the sound velocity, must change with composition and as it changes, affect the thermal conductivity. The linear relationship will be most helpful in predicting the thermal conductivity of new glass compositions.

Examining the absolute values of thermal conductivity for TI #1173, TI #20, As_2Se_3, etc., we find values orders of magnitude below those of crystalline materials. For application with high energy lasers, these low thermal conductivity magnitudes are perhaps the most serious disadvantage of glass materials. Examining the values for sulfur glass composition we can see improvements by a factor of two or three are possible. However, an order of magnitude change does not appear possible.

C. Other Parameters

The thermal change in refractive index for infrared optical materials is experimentally difficult to measure. Results in our own laboratory[29] show that the sign for TI #1173 is positi , but not large, while As_2S_3 is close to zero and negative in sign. Large, excellent quality samples are required to measure the change in refractive index from absolute values measured at different temperatures (the method used in this laboratory). Such measurements are only justified for a fully developed composition and are not discussed here. Discussions of the magnitude and sign relative to materials parameters are found in the literature.[5,29]

The final parameters which decide the worth of a glass for use as melt-formed 10.6 μm laser materials are absorption and thermal stability (relative to devitrification). These two parameters, of course, vary differently within each glass-forming system and cannot be predicted from information presented in this report.

D. Conclusions

1. Compared to selenium-based glasses, the sulfur-based glasses are less dense, have higher glass transition temperatures, lower volume expansion, larger elastic moduli, greater hardness, and higher thermal conductivity.

2. On the basis of the physical parameter data presented here, if one were free to change completely from selenium base to sulfur base, considering only the physical properties, the resulting glass should be harder (+30%) and should have increased elastic moduli (+25%), increased thermal conductivity (+40%), an increase in glass transition temperature (+10%), and a decrease in volume expansion. The degree to which the increase in physical properties can be realized will depend on the absorption at 10.6 μm and the thermal stability of the melt-formed glass.

SECTION IV

GLASSES FROM THE Ge-Sb-S SYSTEM

A. Introduction

Once the decision was reached to prepare and evaluate sulfur-based glasses, the question became: sulfur combined with what elements? The Periodic Table does not represent an inexhaustible supply of possible combinations.[30] The choices are really much more limited than one might expect. For example, the combination of the two-coordinated element sulfur with the three-coordinated element arsenic to form the As_2S_3 glass is well known. However, the physical properties of the resulting glass are rather poor. Previous work at Texas Instruments in an ONR-ARPA funded program[31] dating back over ten years demonstrated the best physical properties are obtained when a four-coordinated group IV A element is combined with a three-coordinated group V A element and a chalcogen to form a ternary system. Attempts in this laboratory to use the group IV B elements and group V B elements in the Transition Element group were unsuccessful.[32] So the choice is limited to Si, Ge, and Sn in the IV A group and P, As, and Sb in the V A group. Elements of the III A group (In and Tl) can be considered, but their use generally leads to high electronic conduction and poor physical properties. Elements in the IB group (Cu, Ag, and Au) were considered because in some bonding situations they are found (especially Cu) to form a four-coordinated structure. However, our attempts to substitute copper and silver in place of the group IV A element failed.

One of the first glass-forming systems evaluated at Texas Instruments under ONR-ARPA sponsorship[31] was the Si-Sb-S system. The combination of silicon with sulfur led to glasses which were chemically unstable and reactive with moisture in the atmosphere. Also, the combination of the light atom silicon with the light atom sulfur led to a high frequency stretching vibration which would limit the use of the glass. Glasses based on the Ge-P-S system were found[31]

to be much more stable, with softening points in excess of 500°C. Unfortunately, the combination of the light element phosphorus with sulfur led to absorption bands in the 8 to 12 μm region. The binary glass Ge_2S_3 was found to transmit to 12 μm, but at that time most infrared systems specified full optical transmission in the 8 to 14 μm range; therefore, that work on sulfur-based glasses was discontinued.

In a recent program at Texas Instruments[23] glasses based on the elements Ge-As-S were evaluated as possible materials for avionics applications. Excellent physical properties were obtained, but as could be expected, absorption typical of As_2S_3 was also observed in the 8 to 14 μm region.

On the basis of all the factors discussed above, the first attempts in this program concentrated on using elements heavier than germanium and arsenic to avoid vibrational modes between constituent elements that would affect the 10.6 μm absorption. Even though previous efforts in this laboratory[31] had yielded glass containing only 10 atom % tin in combination with sulfur, we tried once more to use this IV A element as the basis for a sulfur glass. All samples were found to be crystalline. We finally concluded that the use of the IV A element germanium would be necessary. The conclusion was made to include antimony with germanium in the composition. As reported in Section II of this report, the use of germanium with antimony in TI #1173 produced a better long-wavelength cutoff than the use of germanium with arsenic in TI #20. The conclusion was reached that a glass with a better long-wavelength cutoff would be obtained from the Ge-Sb-S system than with the Ge-As-S system. An additional advantage of antimony relative to arsenic was avoidance of the toxicity problem and the troublesome infrared absorption by the arsenic oxide.

B. Sample Preparation

The methods used in preparing the Ge-Sb-S samples for evaluation were quite similar to those used in the past.[31] The same high purity germanium and antimony

described in Section II, and used to prepare TI #1173, was used in the sulfur experiments. Cominco high purity six-nines sulfur was the third reactant. Small pieces were weighed out to produce a sample of about 40 gms. The reaction tubes were high purity quartz 0.6 inch in diameter and intentionally made quite long (16 to 18 inches). Prior to loading the sample in the tube, the tubes were etched, dried, and pumped out while being heated with a torch to a temperature of 500 to 600°C (surface glows a dull red). The tubes were then cooled and the reactants added. A liquid nitrogen trapped diffusion pump was used to reduce the pressure into the 2×10^{-6} Torr range. Excess moisture and gases dissolved in the sulfur (H_2O and SO_2) were removed by heating the reactants enough to completely melt (without boiling) the granular sulfur. The tubes were then sealed off while still at reduced pressure and placed in the rocking furnace. Six samples at a time were prepared.

Care was exercised during the warm-up period of the reaction step to avoid explosions. The furnace was brought up slowly in temperature to the boiling point of elemental sulfur (450°C). Caution was particularly important for high sulfur glasses (65 to 70 atom %). The reactants were generally allowed to react overnight while rocking at this temperature. The next day, the temperatures were raised slowly upward in 50°C increments. The intention was to try to avoid the effect of a high heat of reaction between the elements which might cause overheating and an explosion. There was some variation in the highest temperature attained. For the high germanium content samples where the relative volatility of the sulfur was very low, the highest liquidus for the Ge-S binary of 850°C was exceeded. For the low germanium compositions where the volatility of the sulfur was high, the highest temperature was 750°C. Rocking continued at the highest temperature for several hours prior to the quench. The quench was accomplished by opening the split furnace and blowing air on the samples. The quench temperature in all cases was 750°C while the samples were in a near upright position. After the samples became solid, they were removed from the

furnace and placed in a quartz-wool insulated chamber and allowed to cool slowly to room temperature. The quartz vials were broken open and the glass pieces removed. Samples of various thicknesses were sawed and polished for evaluation.

C. Results

1. Glass-Forming Region

The results obtained in the evaluation of over 50 compositions are shown in Figure 18. Sample results are designated as crystal, two-phase glass and single-phase glass. Crystalline samples are judged such primarily by their appearance. The appearance is such that the total mass shows facets and the structure of large grain crystals. The two-phase glasses may appear completely amorphous, demonstrate conchoidal fracture, and even have good infrared transmission. However, when examined using the infrared microscope, the materials show two distinct phases on a microscopic or macroscopic scale. In some cases, the entire sample was found to be composed of a uniform glassy matrix with spherical particles embedded in the matrix. In this case, phase separation presumably occurred before the quenching process began.

The single-phase glass, when examined with the infrared microscope, may show some evidence of the presence of a crystalline or crystallite material. The existence of the crystallites depends on the quenching conditions of the individual sample and the location of the composition relative to the glass-forming boundary or key stoichiometric locations such as GeS_2 or Sb_2S_3. However, the crystallites are small and not extensive. One should always keep in mind that the location of the glass boundary as well as the consistency of results within a region are variables subject to the variation of the compounding and quenching conditions. The solid line in Figure 18 encloses the composition region within the Ge-Sb-S system which, under the mild quenching conditions described here, is judged to be amorphous. The dotted line encloses the area

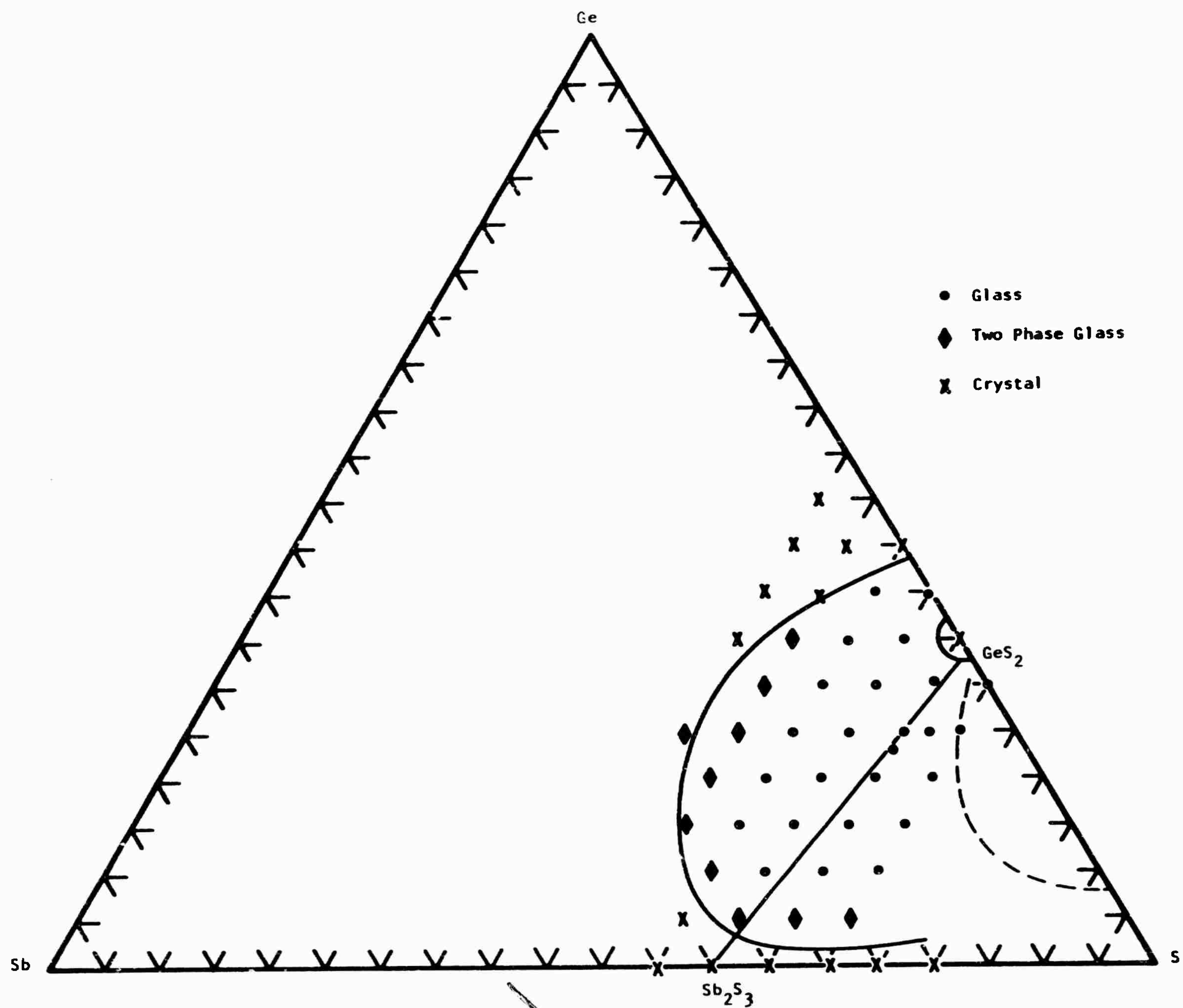

Figure 18 Glass-Forming Composition Diagram for the Ge-Sb-S System

reported in the literature,[33] which we find to be completely in error. Within our region, the best optical properties will be found for glasses within the region of 55 to 65 atom % sulfur.

In the diagram, the stoichiometric compounds GeS_2 and Sb_2S_3 from the two binaries have been connected by a straight line forming a divider between two glass regions where the chemical bonding is different. In the high chalcogen region, all of the bonding requirements for the germanium and the antimony are satisfied by the chalcogen, sulfur. That is, Ge-S and Sb-S bonds form, with the excess sulfur remaining as S-S bonds. On the chalcogen-deficient side of the line, there is competition between the metallic elements for the chalcogen. Thermodynamic considerations may weight the contest heavily in favor of one element over the other (most likely, in favor of germanium over antimony). Nevertheless, because of the relative concentrations involved, some regions can be expected to produce Ge-Ge or Sb-Sb bonds. One may also postulate the formation of distorted geometrical arrangements or even bond-deficient (defect) structures on a local basis. For the chalcogen-deficient composition, the bonding must change from what is considered ordinary arrangements. When this change begins to occur as the stoichiometry line is crossed, changes in the physical properties can also be expected.

From the diagram it is apparent that the binary Sb-S does not form a glass under the compounding and quenching conditions of the experiment. It is interesting to note that the addition of only 5 atom % germanium is enough to pr duce an amorphous material. Admittedly, the material is two-phase glass and probably is not useful as an optical material; nonetheless, it is an amorphous material completely different in appearance from the binary samples. The germanium atom is apparently extremely effective in changing the characteristics of the melt and perhaps increasing the viscosity so that Sb_2S_3 crystallites are unable to form.

2. Physical Properties

Table III lists the measured physical properties for the Ge-Sb-S glass compositions shown in Figure 18. The properties listed are surface hardness, density, glass transition temperature, thermal expansion coefficient, shear and Young's moduli, Poisson's ratio, and thermal conductivity.

Examination of the table reveals that surface hardness above 200 on the Knoop scale is obtained in high germanium glasses. This fact is illustrated in Figure 19 where the hardness measured for the various Ge-Sb-S glasses is plotted versus the atomic % of germanium in the glass. Values for As_2S_3 and TI #1173 are plotted for reference as well.

The densities of the sulfur-based glasses are found to be less than those of the selenium glasses. Figure 20 shows a plot of the measured density for many of the compositions against the calculated molecular weight for each composition. As pointed out in Section II, a linear relationship is observed.

The measured glass transition temperatures listed in the table reach about 360°C. The different regions in terms of T_g's are shown in Figure 21. Lines have been drawn in the glass-forming regions to illustrate glasses with T_g's of 250°C, 300°C, and 350°C. As could be expected, the glass compositions in the highest region lie close to the compound GeS_2 and are low in antimony content.

The volume expansion coefficients are found to be lower than those of selenium glasses and, as pointed out in Section III, are associated with higher T_g's. Figure 22 shows a plot of measured expansion coefficients against the glass transition temperature given in degrees centigrade. Again, a linear relationship is observed.

Table III

Physical Properties of Ge-Sb-S Glasses

Composition Ge	Sb	S	Hardness (Knoop)	Density (gms/cm^3)	Glass Transition Temp. (°C)	Thermal Expansion $\left(\frac{1}{L}\frac{\Delta L}{\Delta T}\ °C \times 10^6\right)$	Shear Modulus (10^6 psi)	Young's Modulus (10^6 psi)	Poisson's Ratio	Thermal Conductivity ($\times 10^4$ W/cm °C)
40	5	55	215	3.39	359	10.1	1.717	4.236	0.234	37
35	10	55	197	3.48	356	10.8	1.521	3.782	0.243	31
35	5	60	198	3.17	363	11.6	1.336	3.347	0.253	30
30	15	55	188	3.57	336	11.4	1.367	3.435	0.257	27
30	10	60	184	3.29	344	11.3	1.211	3.064	0.265	25
30	5	65	183	-	355	13.8	-	-	-	-
25	20	55	174	3.68	313	14.5	1.268	3.206	0.264	25
25	15	60	150	3.41	289	15.5	1.171	2.951	0.261	-
25	10	65	175	3.12	350	13.1	1.053	2.679	0.272	25
25	7.5	67.5	169	3.00	330	13.7	0.992	2.529	0.275	24
23	12	65	167	3.24	287	15.5	1.079	2.743	0.271	23
20	25	55	163	3.81	289	14.5	1.229	3.101	0.262	23
20	20	60	166	3.54	309	13.6	1.126	2.860	0.270	24
20	15	65	156	-	292	16.6	-	-	-	23
15	30	55	154	-	267	15.9	-	-	-	24
15	25	60	148	3.66	256	16.2	1.158	2.925	0.263	25

Table III

(continued)

Composition Ge	Sb	S	Hardness (Knoop)	Density (gms/cm^3)	Glass Transition Temp. (°C)	Thermal Expansion $\left(\frac{1}{L}\frac{\Delta L}{\Delta T}\ °C \times 10^6\right)$	Shear Modulus (10^6 psi)	Young's Modulus (10^6 osi)	Poisson's Ratio	Thermal Conductivity ($x10^4$ W/cm °C)
15	20	65	141	3.43	252	-	1.077	2.742	0.273	23
15	15	70	127	3.20	233	21.7	0.909	2.337	0.286	21
10	30	60	146	2.90	252	16.7	1.260	3.200	0.270	27
10	25	65	134	3.60	-	-	1.123	2.854	0.271	-
5	35	60	138	4.10	234	16.0	1.311	3.312	0.263	27
5	30	65	118	3.79	221	18.4	1.047	2.679	0.280	26
$Ge_{28}Sb_{12}Se_{60}$ (TI #1173)			157	4.40	295	15	1.26	3.17	0.26	22

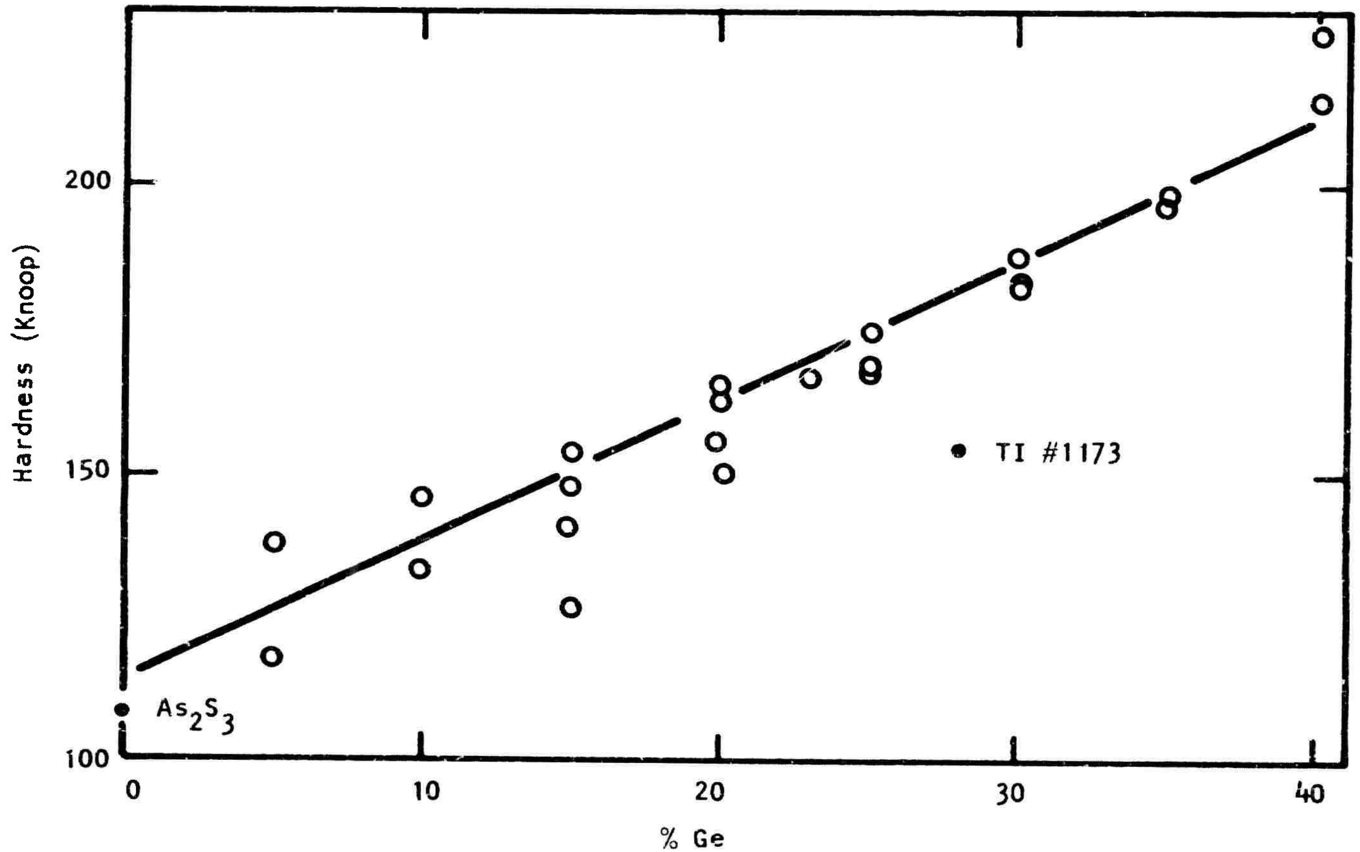

Figure 19 Hardness vs Atom Percent Germanium for Ge-Sb-S Glasses

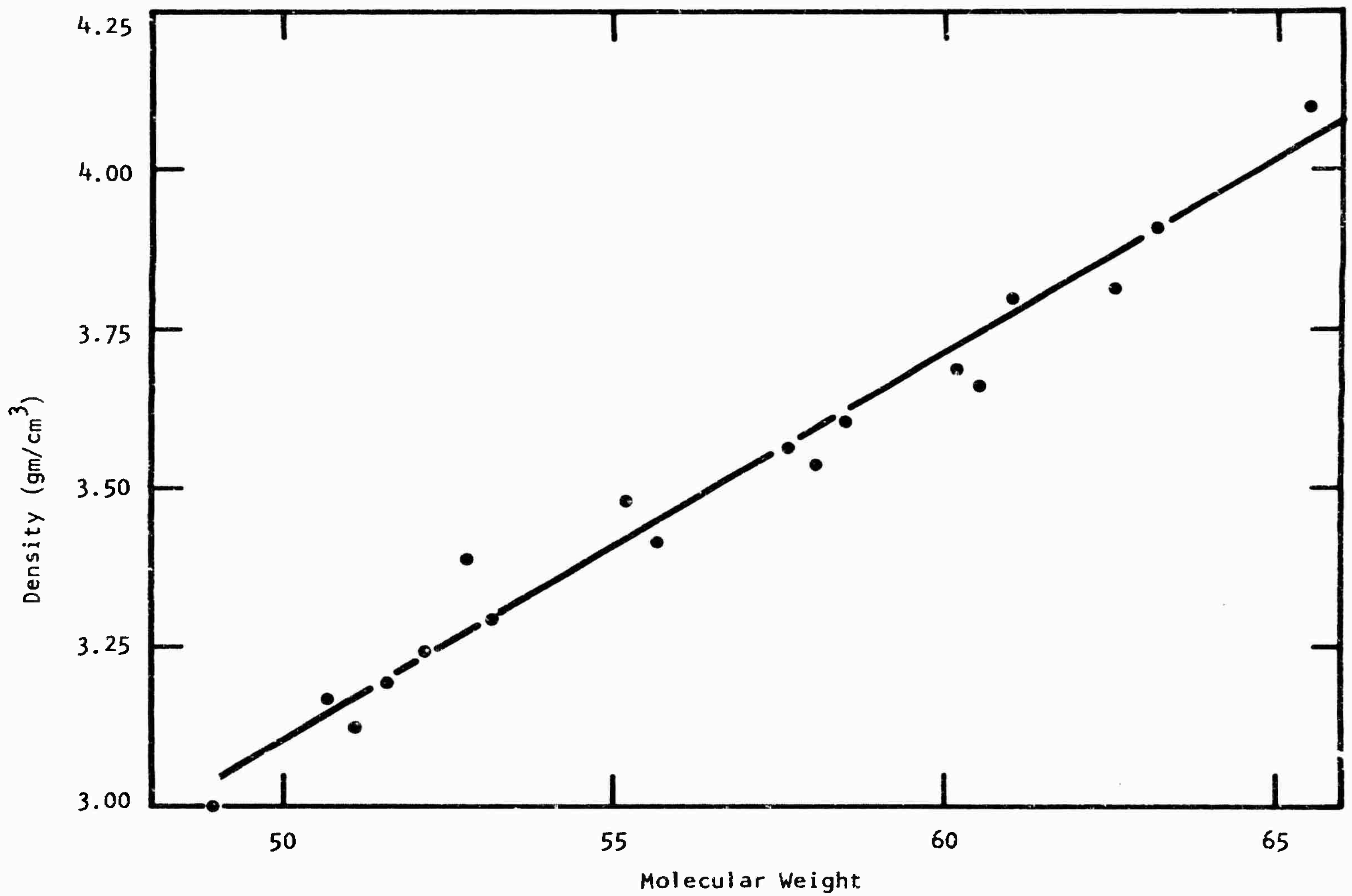

Figure 20 Density as a Function of Molecular Weight for Ge-Sb-S Glasses

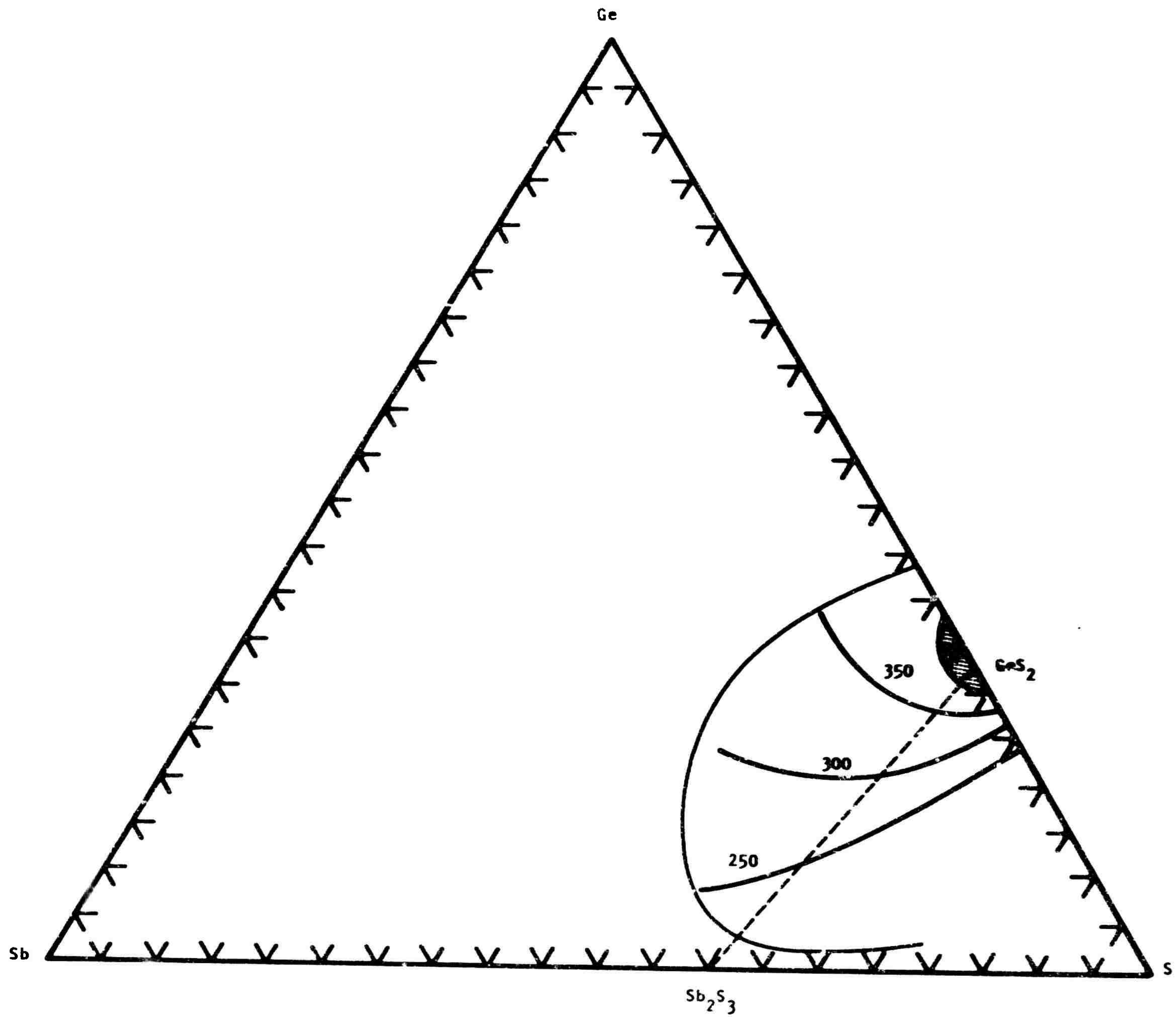

Figure 21 Glass Transition Temperature (T_g °C) Regions for the Ge-Sb-S System

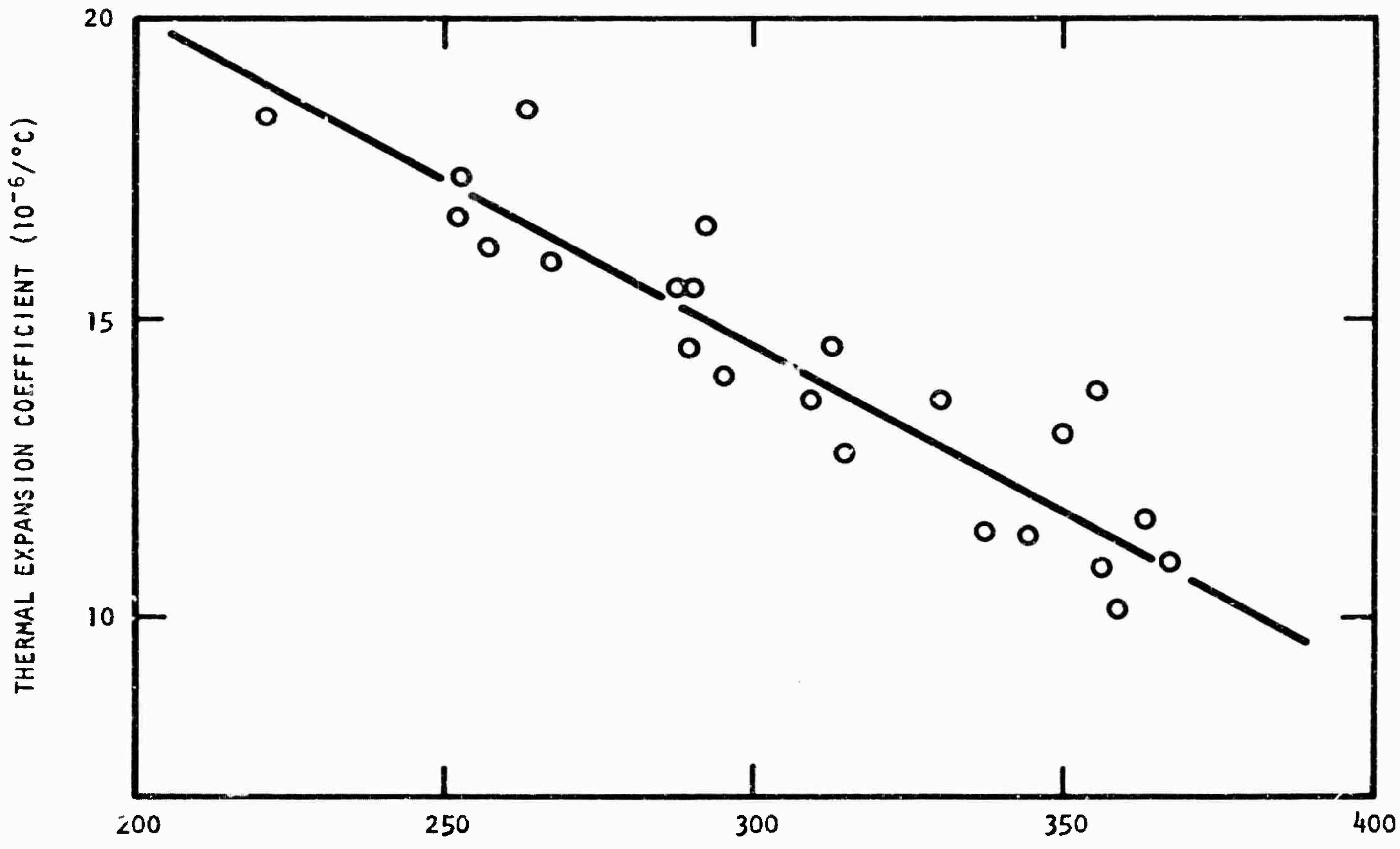

Figure 22 Volume Expansion Coefficients vs T_g's for Ge-Sb-S Glasses

From the values listed in Table III for the shear and Young's modulus, it is apparent that substantial increases were obtained relative to TI #1173. The calculated Poisson's ratios in the table reflect the low values associated with a network structure for the low-sulfur, high-germanium or antimony as compared to the high value typical of a polymeric structure for the high (65 to 70 atom %) sulfur glasses. The listed thermal conductivities are increased about 50% relative to TI #1173 for some useful compositions. Figure 23 again demonstrates the near relationship between thermal conductivity and longitudinal sound velocity as discussed in Section III. From the table it is evident that relative to TI #1173 we can select a glass from the Ge-Sb-S system that will be much harder and more resistant to thermal shock due to increased thermal conductivity and a lower volume expansion coefficient.

3. Optical Properties

The absorption due to constituent atoms in Ge-Sb-S glasses is illustrated in Figure 24. The transmission of very thin samples (~ 0.5 mm thick) for three glasses shown in Figure 24 illustrates the frequencies and changes in the magnitude of absorption for what is believed to be the $2 \times \omega_o$ for Ge-S vibrations and the $2 \times \omega_o$ for Sb-S vibrations. Notice that the strong absorption around 13 μm (770 cm^{-1}) in $Ge_{40}S_{60}$ glass shifts slightly to lower frequency (760 cm^{-1}) in $Ge_{25}Sb_{15}S_{60}$ glass and $Ge_5Sb_{35}S_{60}$ glass. The absorption due to Sb-S vibrations is completely absent, of course, in the $Ge_{40}S_{60}$ glass, but appears around 16 μm (615 cm^{-1}) in the low antimony glass, $Ge_{25}Sb_{15}S_{60}$, shifting to lower frequency (605 cm^{-1}), and becomes a stronger absorption in $Ge_5Sb_{35}S_{60}$ glass. The changes in magnitude with composition for the Ge-S vibration are illustrated in Figure 25, where the absorption coefficient around 13 μm calculated from measured transmission of two thin pieces is plotted as a function of germanium content of the glass. An almost linear relation is shown. The same type of treatment for

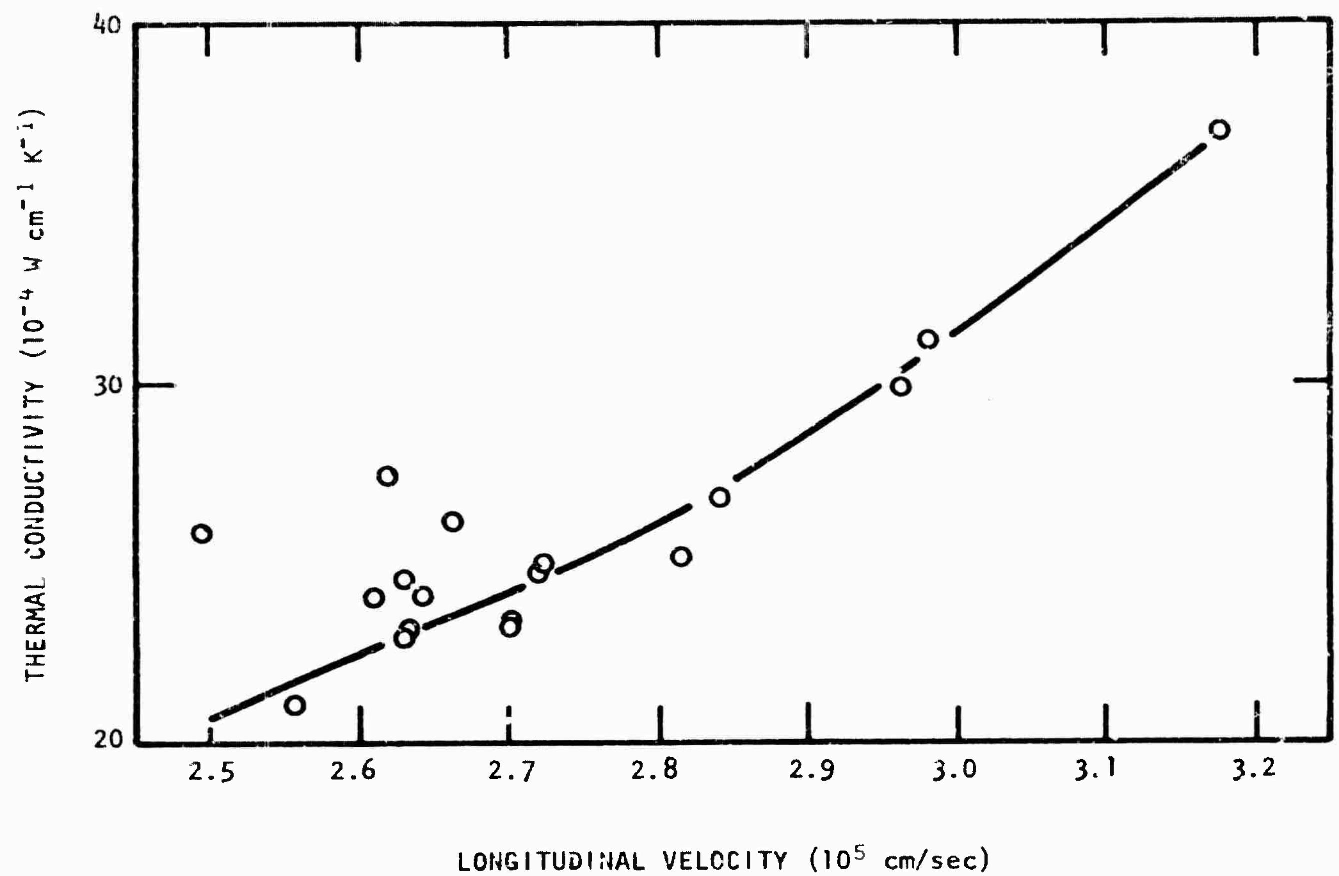

Figure 23 Thermal Conductivity vs Longitudinal Sound Velocity for Ge-Sb-S Glasses

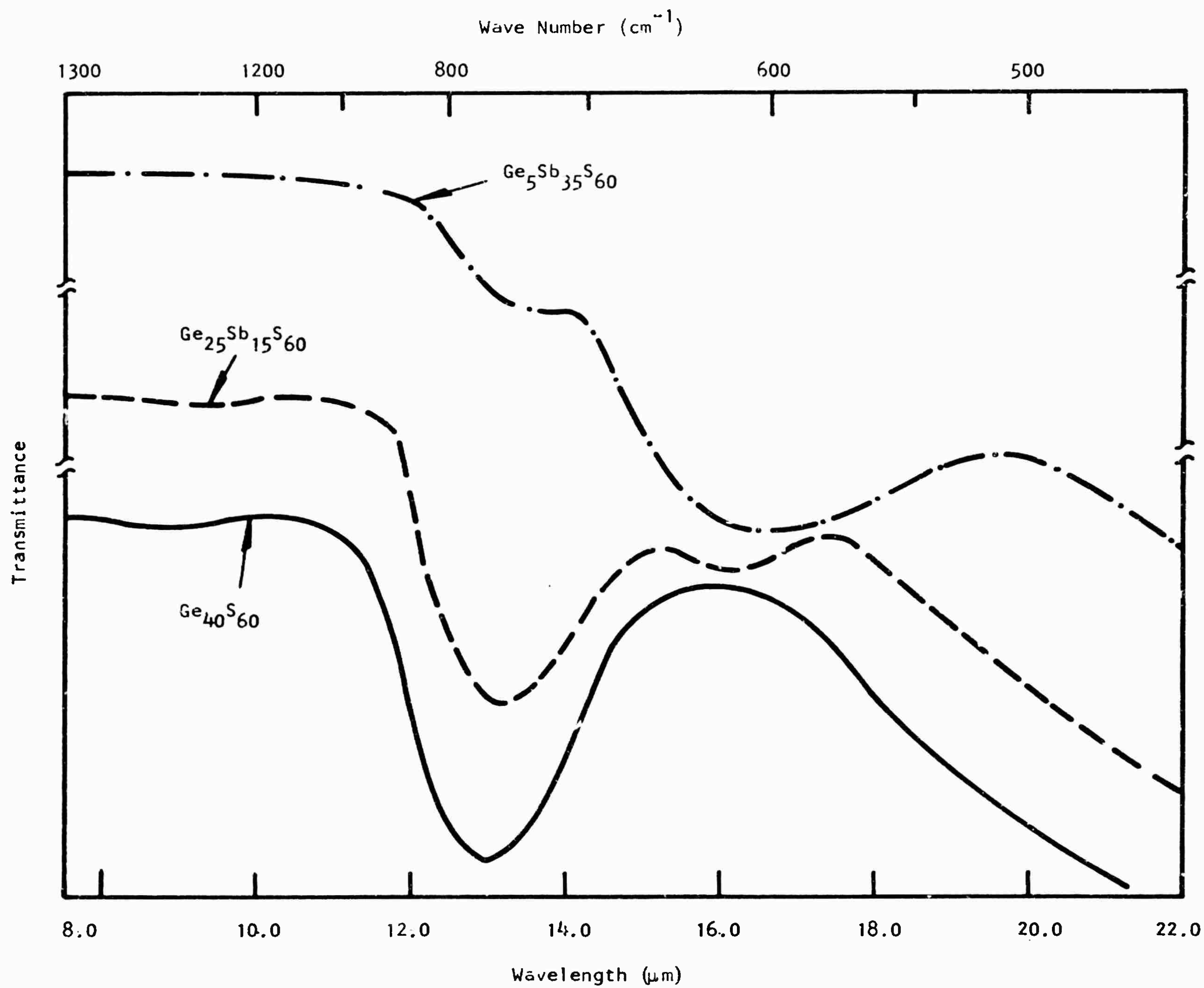

Figure 24 Measured Infrared Transmission for Some Thin Slices of Ge-Sb-S Glasses

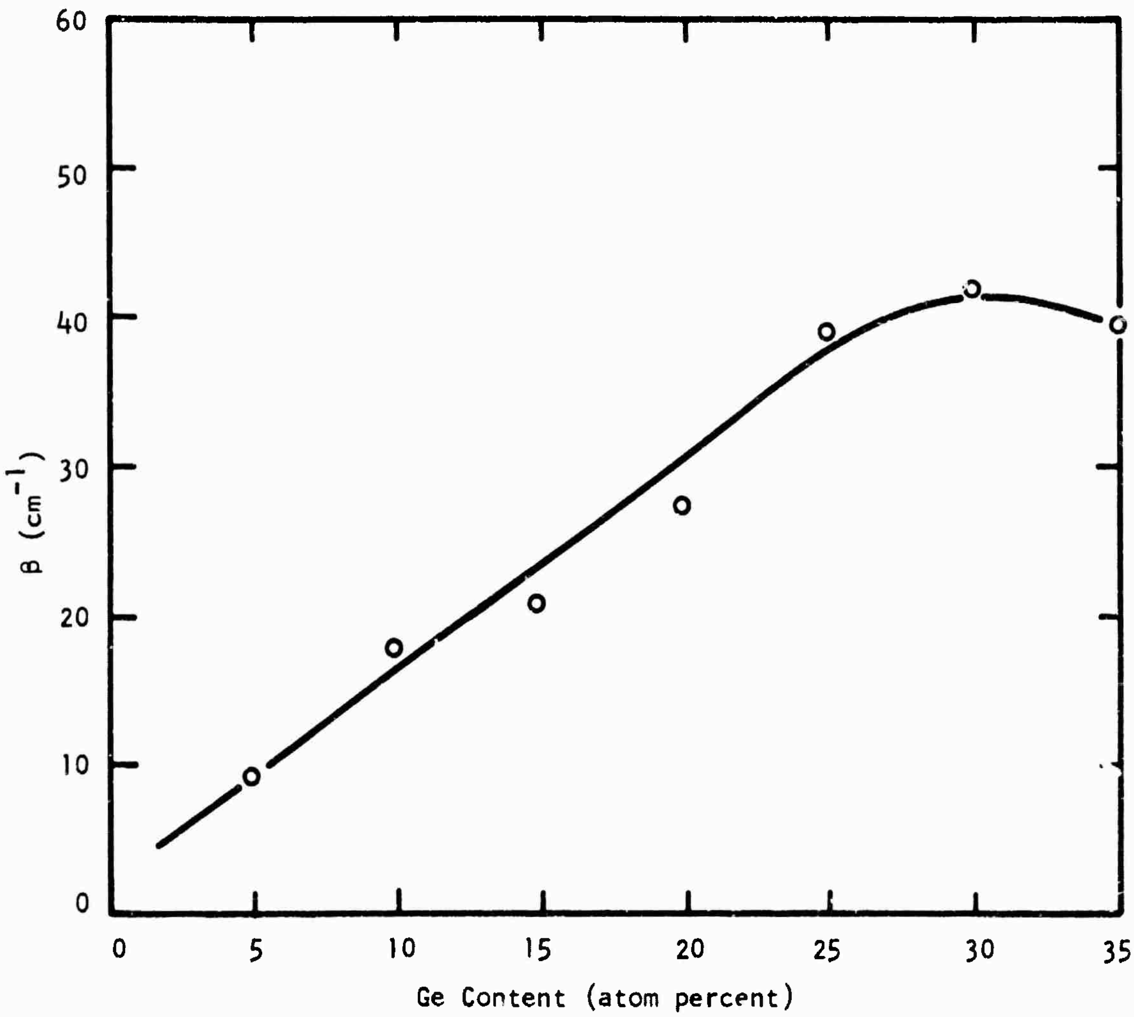

Figure 25 Absorption at 13 μm as a Function of Germanium Content in Ge-Sb-S Glasses

the Sb-S vibration is illustrated in Figure 26, where the calculated absorption coefficient around 16 μm is plotted against antimony content of the glass. Again, an almost linear relation is obtained.

Limitations in the long wavelength transmission for Ge-Sb-S glasses are illustrated in Figure 27 where the measured transmission for 1 cm thick samples of $Ge_{30}Sb_{10}S_{60}$ (analogous to a sulfur version of TI #1173), $Ge_{10}Sb_{30}S_{60}$ (low germanium - high antimony glass) and $Ge_{15}Sb_{15}S_{70}$ (high sulfur content) are presented. First, note that all three glasses transmit visible light. They all suffer from slight absorption around 4 μm, which is presumably due to dissolved H_2S. The high germanium glass demonstrates broad, strong absorption around 9 μm (1110 cm^{-1}), presumably due to the third order Ge-S vibration. In the low germanium - high antimony glass, the third order Ge-S is very broad and much weaker, appearing as a shoulder on the long wavelength cutoff for the glass. The high sulfur glass shows an additional absorption at 7.65 μm (1310 cm^{-1}), which we believe to be the third order S-S vibration. In addition, note that there is no absorption we can attribute to the third order Sb-S vibration, which should occur around 11 μm (900 cm^{-1}) judging by the second order frequency and the first order (280 cm^{-1}) reported in the literature.[34] The point has been made many times before that quantitative judgments based on results obtained from the evaluation of small samples are often in error. Careful preparation of large batches (1 kgm) using the methods discussed in Section II will be necessary before we can accurately predict the long wavelength cutoff for this system. For example, germanium oxide and the third order Sb-S both seem to absorb at frequencies close to the second order Ge-S vibration. This fact is illustrated in Figure 28 in the exponential decay plots for $Ge_{30}Sb_{10}S_{60}$ and $Ge_{10}Sb_{30}S_{60}$ compared to TI #1173. The absorption around 770 cm^{-1} for $Ge_{30}Sb_{10}S_{60}$ seems too large for a second order process. Oxide contribution is expected to account for a large amount of this absorption and to affect the 10.6 μm level. The magnitude of the level at 10.6 μm for the glasses presented in this diagram is of the order of 0.5 cm^{-1}.

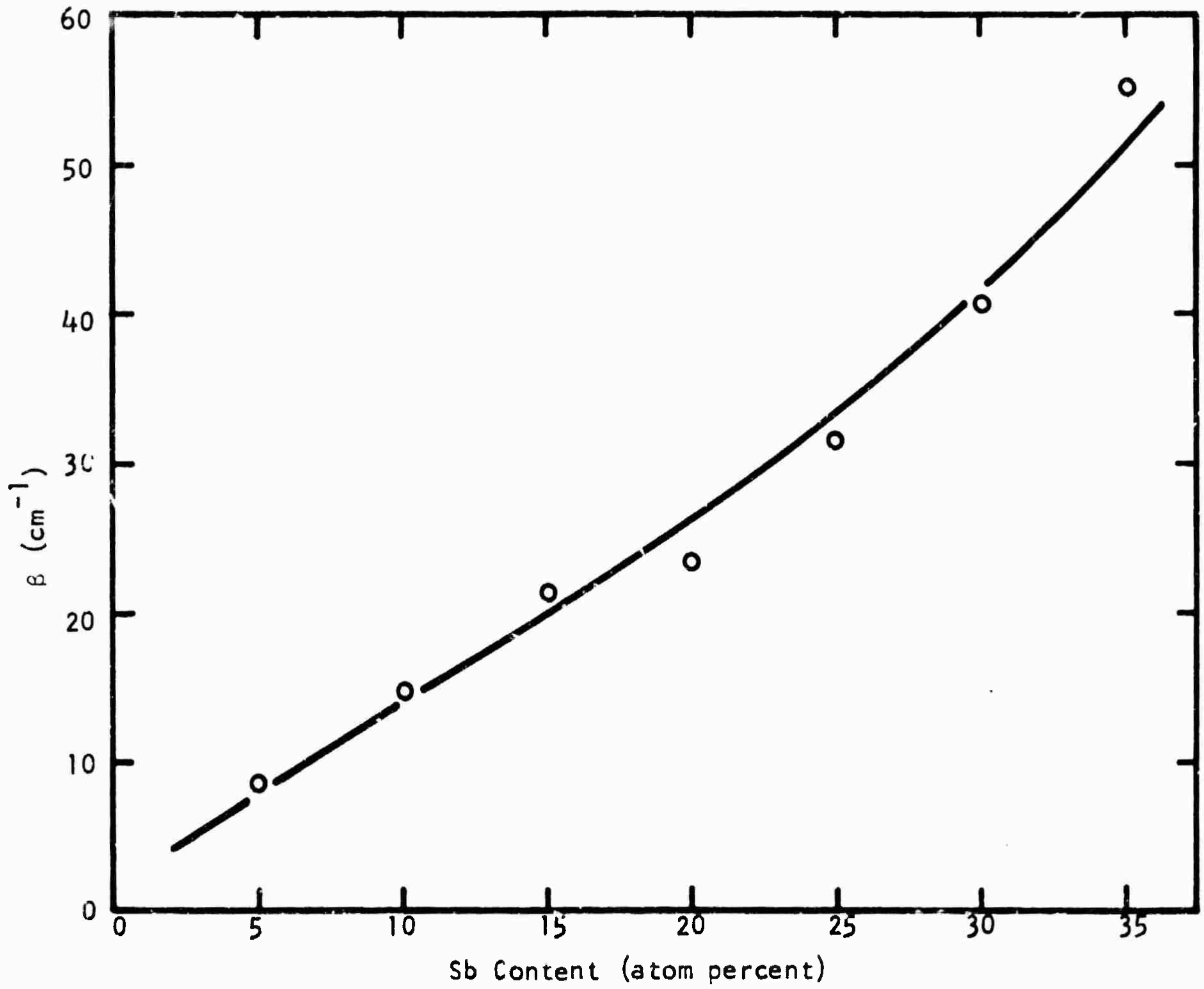

Figure 26 Absorption at 16 μm as a Function of Antimony Content in Ge-Sb-S Glasses

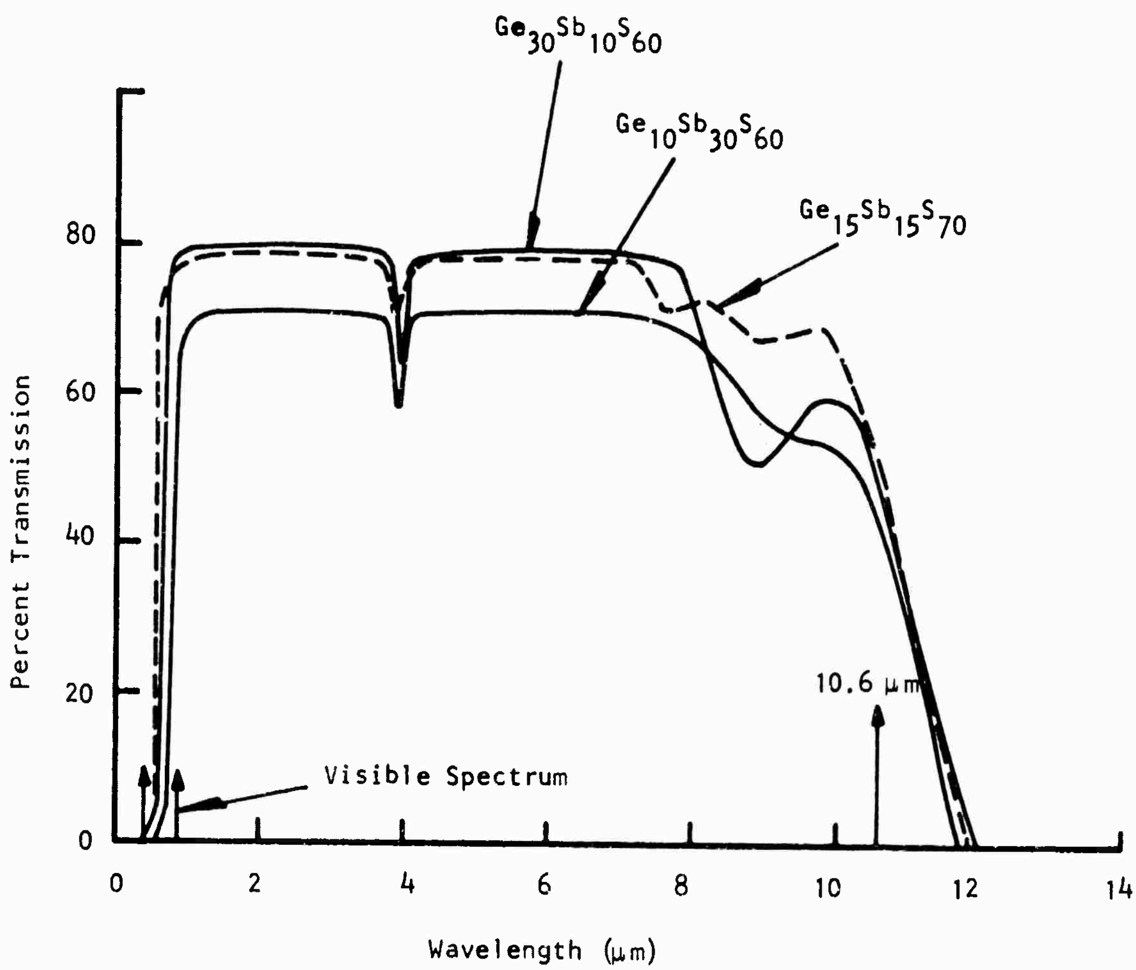

Figure 27 Measured Transmission of 1 cm Samples of Ge-Sb-S Glasses

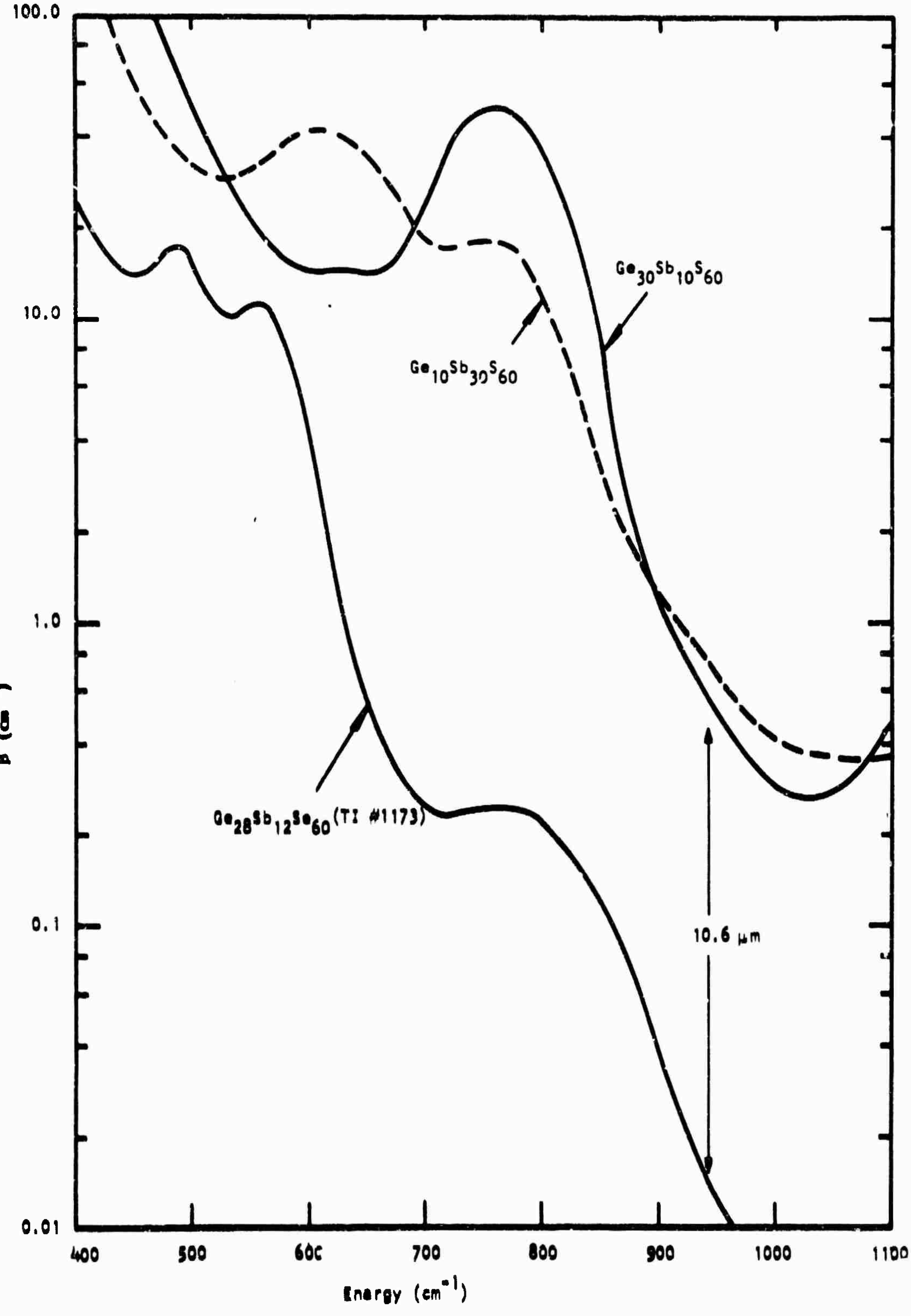

Figure 28 Exponential Absorption Plot for Ge-Sb-S Glasses Compared to TI #1173

The optical values for most of the Ge-Sb-S glasses characterized are presented in Table IV. The first column lists the wavelength location of the absorption edge for each composition as determined by transmission plots obtained using very thin samples. Thus, the values represent extrapolation from the steep, high magnitude portion of the absorption edge. Visible transmission is obtained for most compositions in which the sulfur content is 60 atom % or greater. This fact is illustrated in Figure 29, where the data from Table IV have been plotted in terms of atomic percent sulfur against wavelength location of the absorption edge. The visible light portion of the spectrum (0.4 to 0.8 μm) has been added for reference along with the wavelength (1.06 μm) of the YAG laser used as a target designator source (important wavelength from the standpoint of avionics systems). From the diagram, it is evident that visible transmission is typical of the chalcogen-rich polymeric glasses. As the sulfur content drops below 60 atom % around the stoichiometry line, the visible transmission is lost. Perhaps the loss in visible transmission reflects the appearance of Ge-Ge bonds (absorption edge in germanium occurs at 2 μm) or formation of Sb-Sb bonds (metallic in character with no IR transmission) necessary for the emergence of the network structure.

All the absorption values listed in Table IV were obtained by the measured IR transmission of thin (~ 0.3 cm) and thick (~ 1 cm) samples. The first column, listed as 7.65 μm (1310 cm^{-1}), was included to indicate the existence of the higher order sulfur absorption due to the presence of polymeric structure. The absorption is noticeable when the sulfur content is about 65 atom % and increases with increasing sulfur content. The magnitude also depends on the Ge/Sb ratio.

The value included at 8 μm indicates to some extent the quality of the sample. At this wavelength point, the glass should have a low absorption value, of the order of 0.01 to 0.03 cm^{-1}. Failure to obtain this value indicates the quality is not too good due to strain, inclusions, cracks, bubbles, etc.

Table IV

Calculated Absorption Coefficients in cm^{-1} and Absorption Edge Wavelengths for Ge-Sb-S Glasses

Composition Ge	Sb	S	Absorption Edge (μm)	β at 7.65 μm	β at 8 μm	β at 9 μm	β at 10 μm	β at 10.6 μm	β at 11 μm
40	5	55	0.75	-	0.13	0.53	0.31	0.72	1.2
35	10	55	0.86	-	0.03	0.48	0.27	0.49	0.85
35	5	60	0.64	-	0.09	0.65	0.30	0.65	1.2
30	15	55	0.90	-	0.06	0.44	0.30	0.54	0.82
30	10	60	0.66	-	0.08	0.45	0.27	0.57	0.95
25	20	55	0.84	-	0.13	0.33	0.30	0.54	0.85
25	15	60	0.67	-	0.06	0.56	0.36	0.62	1.0
25	10	65	0.53	-	0.3	0.76	0.54	0.91	1.2
20	25	55	0.90	-	0.06	0.36	0.29	0.52	0.82
20	20	60	0.69	-	0.05	0.4	0.27	0.60	1.0
20	15	65	0.53	-	0.3	0.49	0.60	0.91	1.4
15	30	55	0.95	-	0.12	0.31	0.30	0.56	0.77
15	25	60	0.73	-	0.08	0.35	0.35	0.70	1.1
15	20	65	0.59	0.1	0.15	0.40	0.45	1.2	1.6
15	15	70	0.56	0.3	0.19	0.37	0.56	1.6	2.1
10	30	60	0.72	-	0.15	0.35	0.40	0.75	1.1
10	20	70	-	0.6	0.09	0.23	0.35	1.3	1.9
5	35	60	0.88	-	0.14	0.36	0.47	1.2	1.7
5	30	65	-	0.3	0.18	0.22	0.52	1.2	1.3

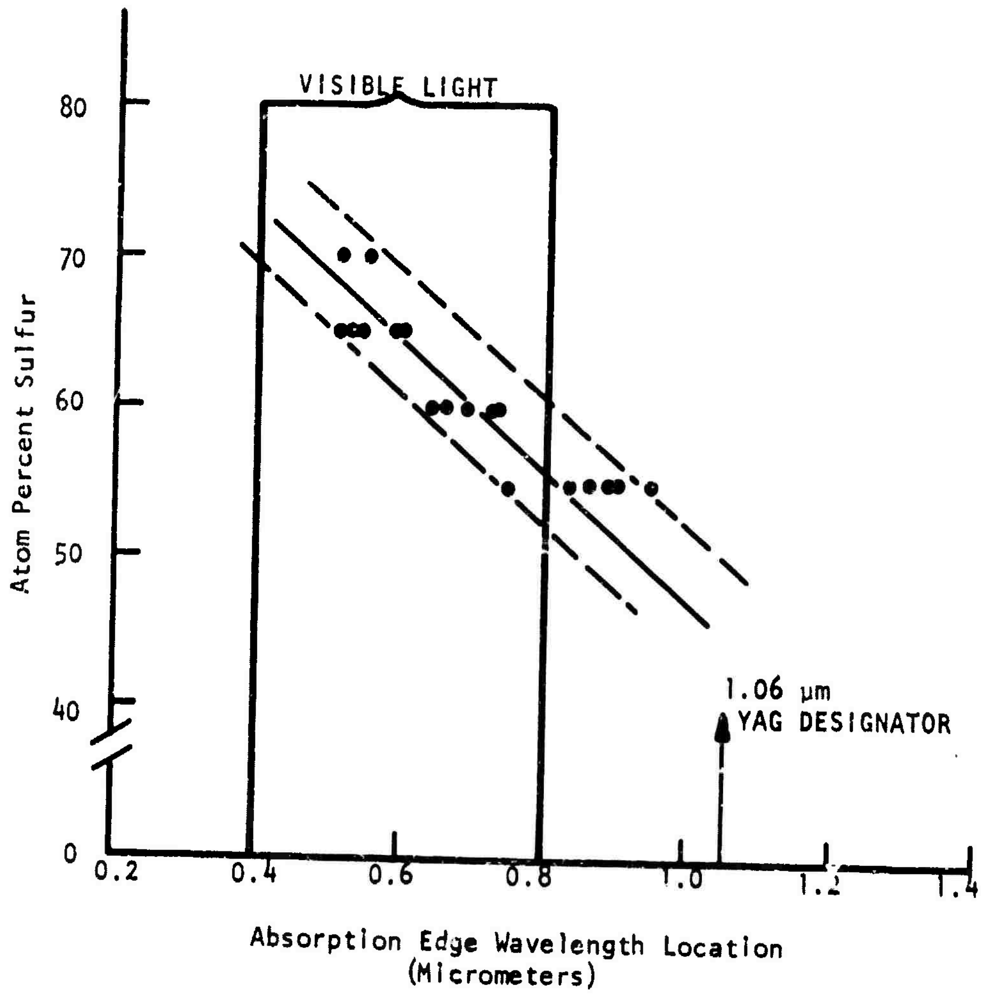

Figure 29 Absorption Edge Wavelength Location as a Function of Sulfur Content in Ge-Sb-S Glasses

Values at 9 μm indicate the strength of the third order Ge-S vibration. There is a fair correlation between this magnitude and the germanium content, but the picture is complicated by silicon-oxygen impurities. As mentioned for TI #1173 in Section II, the Si-O stretch occurs around 9.5 μm.

The 10 μm and 11 μm values were added to indicate levels on both sides of the 10.6 μm value of the CO_2 laser. From Table IV, one may conclude the level in Ge-Sb-S glasses for small samples is around 0.5 cm^{-1}. For large, high purity samples one might predict that a level of 0.1 cm^{-1} will be reached. But certainly, the level of 0.01 to 0.001 cm^{-1} predicted for Ge-Sb-Se glasses will not be approached.

D. Discussion of Results

The results presented concerning the physical and optical properties of Ge-Sb-S glasses are based on small samples prepared without the benefit of reactant purification steps. For this reason, the optical results are to some degree transitory and will have to stand until large batches of a few compositions can be prepared and evaluated in detail. Such questions as intrinsic long wavelength limit, change in refractive index with temperature, and limiting absorption coefficient at 10.6 μm can only be guessed at this point. It is unfortunate that the period of this contract ended before the necessary information could be obtained to include in this report. However, work on this system will continue using company funds, and the final results will be reported elsewhere.

E. Conclusions

1. The physical properties of glasses based on sulfur are considerably better than those of the selenium-based glasses relative to their application as infrared optical materials.

2. The long wavelength cutoff for Ge-Sb-S glasses is determined by higher order vibration of the constituent atoms, similar to the case of Ge-Sb-Se glasses.

3. Results obtained from small laboratory samples indicate the absorption level for Ge-Sb-S glasses is about 0.5 cm^{-1}. Removal of silicon-oxygen and germanium-oxygen impurities may decrease this value to the 0.1 cm^{-1} range. The exact intrinsic limit for these materials is not known at this time.

SECTION V

CONCLUSIONS

The overall purpose of this program was to investigate the suitability of chalcogenide glasses for application with high energy CO_2 lasers. The two major disadvantages for the glass materials were identified as low thermal conductivity and high absorption (high relative to the 0.0001 cm^{-1} level of alkali halides). The following conclusions can be drawn from the information presented in this report:

1. The intrinsic absorption limit for selenium-based glasses at 10.6 μm is in the 0.001 to 0.01 cm^{-1} range. This level appears to be at least as large as, and perhaps larger than, the level for crystalline compounds based on selenium with fundamental lattice frequencies of about the same order. The appearance of second order and third order peaks at the long wavelength limit indicates glasses are susceptible to higher order absorption processes, probably due to the anharmonic nature of their vibrations.

2. The related physical properties of thermal conductivity, volume expansion, and thermal change in refractive index (as indicated by the location of the absorption edge) can be improved by switching to a sulfur-based glass in place of selenium. However, the price paid is higher frequency vibrations by constituent atoms leading to a movement of the long wavelength cutoff toward the 10.6 μm wavelength. An estimate of the intrinsic limit for sulfur-based glasses at 10.6 μm is in the 0.05 to 0.1 cm^{-1} range. The one to two orders of magnitude increase in absorption at 10.6 μm is not offset by the fractional improvements in related physical properties.

3. One might speculate that substantial reduction in absorption at 10.6 μm may be obtained if the basis of the glass is switched to the heavier chalcogen atom, tellurium. Lower frequency vibrations between constituent atoms would

lead to a long wavelength cutoff substantially removed from 10.6 μm. However, the price paid would be lower thermal conductivity, and a greater positive dN/dT, judging by the absorption edge movement to longer wavelength. Possibly, the 10.6 μm level would also come under the influence of the Urbach tail at the absorption edge.

4. For the high energy CO_2 laser, the chalcogenide glasses do not appear promising as a window materials.

REFERENCES

1. A. R. Hilton and M. J. Brau, Infrared Physics 3, 67-76 (1963).
2. Proceedings of Conference on High Power Infrared Laser Window Materials, Air Force Cambridge Research Laboratories, edited by Charles Sahagian and Carl Pitha, October 27-28, 1971.
3. Proceedings of Conference on High Power Infrared Laser Window Materials, Air Force Cambridge Research Laboratories, edited by Carl Pitha, October 30 - November 1, 1973.
4. A. R. Hilton, Journal of Electronic Materials 2, 211 (1973).
5. B. Bendow, Journal of Electronic Materials 3, 101 (1974).
6. W. Kaiser and P. H. Keck, J. Appl. Phys. 28, 882 (1957).
7. A. Vasko, D. Lezal, and I. Srb, J. Non-Cryst. Sol. 4, 311 (1970).
8. A. R. Hilton, H. C. Hafner, and R. L. Rasmussen, Conference on High Power Infrared Laser Window Materials, Vol. II, pp. 693-704, 1972.
9. E. A. Schweikert and H. L. Rook, Anal. Chem. 42, 1525 (1970).
10. For TI #1173, A. R. Hilton and C. E. Jones, Appl. Optics 6, 1513 (1907). For TI #20, H. C. Hafner and C. E. Jones, Texas Instruments Inc., private communication.
11. M. Hass, Naval Research Laboratory, "High Energy Laser Windows," Semiannual Report No. 1, December 1972.
12. D. A. Pinnow and T. C. Rich, Appl. Optics 12, 984 (1973).
13. M. Hass, Naval Research Laboratory, Washington D.C., private communication.
14. P. Macedo, Catholic University, Washington D.C., private communication.
15. Samples from J. Adams, Eagle Picher Corporation, Quapah, Oklahoma.
16. C. E. Jones and H. C. Hafner, "Research on Infrared Optical Materials", Contract AFAL-TR-68-348, Air Force Avionics Laboratory, Wright-Patterson Air Force Base, January 1969.
17. G. Lucovsky, A. Mooradian, W. Taylor, G. B. Wright, and R. C. Keezer, Solid State Commun. 5, 113 (1967).
18. V. A. Twaddell, W. C. LaCourse, and J. D. Mackenzie, J. Non-Cryst. Sol. 8, 831 (1972).
19. J. Tauc and A. Menth, J. Non-Cryst. Sol. 8, 569 (1972)
20. "Integrated Injection Laser-Waveguide Device," Contract N00014-73-C-0288, Office of Naval Research, Washington, D.C.

REFERENCES

(continued)

21. M. Sparks, J. Appl. Phys. 42, 5029 (1971).

22. A. R. Hilton, C. E. Jones, and M. J. Brau, Phys. Chem. Glasses 7, 105 (1966).

23. H. C. Hafner, "Development of Infrared Glass for Reconnaissance and Weapon Delivery," Contract F33615-72-C-1887, Air Force Avionics Laboratory, Wright-Patterson Air Force Base, Ohio.

24. K. A. Gschneider, Solid State Physics, Vol. 16, ed. by Fredrick Seitz and David Turnbull (Academic Press, New York, 1964).

25. S. Sakka and J. D. Mackenzie, J. Non-Cryst. Sol. 6, 145 (1971).

26. J. T. Krause, C. R. Kurkjian, D. A. Pinnow, and E. Sigety, Appl. Phys. Lett. 17, 367 (1970).

27. L. Stourac, A. Vasko, I. Srb, C. Musil and F. Strba, Czech. J. Phys. B18, 1067 (1968).

28. V. E. Schnaus and C. T. Moynihan, Mater. Sci. Engr. 7, 268 (1971).

29. A. R. Hilton and C. E. Jones, Appl. Opt. 6, 1513 (1967).

30. A. R. Hilton, Phys. Chem. Glasses 9, 148 (1968).

31. "Final Technical Summary Report for New High Temperature Infrared Transmitting Glasses," May 1962 - July 1965, Office of Naval Research Contract NONR 3810(00), A. R. Hilton, Texas Instruments Incorporated, September 1965.

32. "Final Technical Summary Report for Titanium Chalcognide Infrared Transmitting Glasses," Office of Naval Research Contract No. N00014-66-C0085, A. R. Hilton, Texas Instruments Incorporated, February 1967.

33. I. D. Turjanitsa, I. M. Miholinets, B. M. Koperljos, and I. F. Kopinets, J. Non-Cryst. Sol. 11, 173 (1972).

34. Von V. Riede, Ann. Phys. 7, 415 (1970).